

# QUANTUM CHROMODYNAMICS

*G. Ecker*

Inst. Theor. Physics, Univ. of Vienna, Austria

## Abstract

After a brief historical review of the emergence of QCD as the quantum field theory of strong interactions, the basic notions of colour and gauge invariance are introduced leading to the QCD Lagrangian. The second lecture is devoted to perturbative QCD, from tree-level processes to higher-order corrections in renormalized perturbation theory, including jet production in  $e^+e^-$  annihilation, hadronic  $\tau$  decays and deep inelastic scattering. The final two lectures treat various aspects of QCD beyond perturbation theory. The main theme is effective field theories, from heavy quarks to the light quark sector where the spontaneously broken chiral symmetry of QCD plays a crucial role.

## Table of contents

1	Introduction . . . . .	2
1.1	Historical background . . . . .	2
1.2	Colour . . . . .	5
1.3	Gauge invariance . . . . .	6
1.4	$SU(3)_c$ and the QCD Lagrangian . . . . .	7
2	Perturbative QCD . . . . .	10
2.1	QCD at tree level . . . . .	10
2.2	Higher-order corrections and renormalization . . . . .	13
2.3	Measurements of $\alpha_s$ . . . . .	16
2.4	Hadronic $\tau$ decays . . . . .	18
2.5	Deep inelastic scattering . . . . .	19
3	Heavy and light quarks . . . . .	25
3.1	Effective field theories . . . . .	25
3.2	Heavy quarks . . . . .	26
3.3	QCD sum rules . . . . .	29
3.4	Chiral symmetry . . . . .	33
3.5	Chiral perturbation theory . . . . .	37
3.6	Light quark masses . . . . .	40
3.7	Pion pion scattering . . . . .	42
3.8	$K_{l3}$ decays and $V_{us}$ . . . . .	43
4	Summary and epilogue . . . . .	46
	References . . . . .	46

# 1 Introduction

Why do we still study QCD after more than 30 years?

- By decision of the Nobel Prize Committee in 2004 [1], QCD is the correct theory of the strong interactions.
- The parameters of QCD, the coupling strength  $\alpha_s$  and the quark masses, need to be measured as precisely as possible.
- Electroweak processes of hadrons necessarily involve the strong interactions.
- In searches for new physics at present and future accelerators, the “QCD background” must be understood quantitatively.
- Although QCD is under control for high-energy processes, many open questions remain in the nonperturbative domain (confinement, chiral symmetry breaking, hadronization, . . . )
- Last but not least, QCD is a fascinating part of modern physics. The lectures will therefore start with a brief historical review of the developments in particle physics in the sixties and early seventies of the last century.

The following lectures were given to an audience of young experimental particle physicists. Although the lectures emphasize some of the theoretical aspects of QCD, the mathematical level was kept reasonably low. The first two lectures cover the basics of QCD, from the concepts of colour and gauge invariance to some applications of perturbative QCD. The last two lectures treat aspects of QCD beyond perturbation theory. The main theme is effective field theories, from heavy quarks to the light quark sector where the spontaneously broken chiral symmetry plays a crucial role.

## 1.1 Historical background

Particle physics in the early sixties of the last century was not in a very satisfactory state. Only for the electromagnetic interactions of leptons a full-fledged quantum field theory (QFT) was available. Quantum electrodynamics (QED) produced increasingly precise predictions that were confirmed experimentally. Nevertheless, the methodology of renormalization, an essential aspect of the perturbative treatment of QED, was not universally accepted. Even among the founding fathers of QFT, the dissatisfaction with “sweeping the infinities under the rug” was widespread. At the Solvay Conference of 1961, Feynman confessed [2] that he did not “subscribe to the philosophy of renormalization”.

What is the essence of this controversial procedure of renormalization that has turned out to be crucial for the shaping of QCD and of the Standard Model altogether? Specializing to QED for definiteness, three main steps are important.

- Amplitudes  $A(p_i; e_0, m_0; \Lambda)$  depend on the momenta  $p_i$  of the particles involved, on the parameters  $e_0, m_0$  of the QED Lagrangian and on a cutoff  $\Lambda$  that cuts off the high-momentum modes of the theory. The cutoff is essential because  $A(p_i; e_0, m_0; \Lambda)$  diverges for  $\Lambda \rightarrow \infty$ , rendering the result meaningless.
- With the help of measurable quantities (cross sections, particle four-momenta) one defines physical parameters  $e(\mu), m(\mu)$  that depend in general on an arbitrary renormalization scale  $\mu$ . One then trades  $e_0, m_0$  for the physical  $e(\mu), m(\mu)$  to a given order in perturbation theory.
- The limit  $\lim_{\Lambda \rightarrow \infty} A(p_i; e_0(e, m, \Lambda), m_0(e, m, \Lambda); \Lambda) = \hat{A}(p_i; e(\mu), m(\mu))$  is now finite and unambiguous for the chosen definitions of  $e(\mu), m(\mu)$ .

Based on this procedure, the agreement between theory and experiment was steadily improving.

For the weak interactions, the Fermi theory (in the  $V - A$  version) was quite successful for weak decays, but

- higher-order corrections were not calculable;
- for scattering processes the theory became inconsistent for energies  $E \gtrsim 300$  GeV (unitarity problem).

The rescue came at the end of the sixties in the form of the electroweak gauge theory of the Standard Model.

Of all the fundamental interactions, the strong interactions were in the most deplorable state. Although the rapidly increasing number of hadrons could be classified successfully by the quark model of Gell-Mann and Zweig [3], the dynamics behind the quark model was a complete mystery. A perturbative treatment was clearly hopeless and the conviction gained ground that QFT might not be adequate for the strong interactions.

This conviction was spelled out explicitly by the proponents of the bootstrap philosophy (Chew et al.). Under the banner of nuclear democracy, all hadrons were declared to be equal. Instead of looking for more fundamental constituents of hadrons, the S-matrix for strong processes was investigated directly without invoking any quantum field theory. Although the expectations were high, nuclear democracy shared the fate of the student movement of the late sixties: the promises could not be fulfilled.

A less radical approach assumed that QFT could still be useful as a kind of toy model. The main proponent of this approach was Gell-Mann who suggested to abstract algebraic relations from a Lagrangian field theory model but then throw away the model (“French cuisine program” [4]). The usefulness of this approach had been demonstrated by Gell-Mann himself: current algebra and the quark model were impressive examples. Until the early seventies, Gell-Mann took his program seriously in declaring the quarks to be purely mathematical entities without any physical reality, a view shared by many particle physicists of the time.

The decisive clue came from experiment. Started by the MIT-SLAC collaboration at the end of the sixties, deep inelastic scattering of leptons on nucleons and nuclei produced unexpected results. Whereas at low energies the cross sections were characterized by baryon resonance production, the behaviour at large energies and momentum transfer was surprisingly simple: the nucleons seemed to consist of noninteracting partons (Feynman). Obvious candidates for the partons were the quarks but this idea led to a seeming paradox. How could the quarks be quasi-free at high energies and yet be permanently bound in hadrons, a low-energy manifestation?

That the strength of an interaction could be energy dependent was not really new to theorists. In QED, the vacuum acts like a polarisable medium leading to the phenomenon of charge screening. However, contrary to what the deep inelastic experiments seemed to suggest for the strong interactions, the effective charge in QED increases with energy: QED is ultraviolet unstable.

To understand the phenomenon of an energy dependent interaction, we consider the dimensionless ratio of cross sections

$$R_{e^+e^-} = \frac{\sigma(e^+ + e^- \rightarrow \text{hadrons})}{\sigma(e^+ + e^- \rightarrow \mu^+ + \mu^-)} . \quad (1)$$

Beyond the leading-order value  $R_0$  (cf. Sec. 2.1), one finds to lowest order in the strong coupling constants  $g_s$ :

$$R_{e^+e^-} = R_0 \left( 1 + \frac{g_s^2}{4\pi^2} \right) . \quad (2)$$

The general form to any order in  $g_s$  (neglecting quark masses) is

$$R_{e^+e^-} = R_{e^+e^-}(E, \mu, g_s(\mu)) \quad (3)$$

where  $E$  is the center-of-mass energy and  $\mu$  is the renormalization scale. Since  $R_{e^+e^-}$  is a measurable quantity, it must be independent of the arbitrary scale  $\mu$ :

$$\mu \frac{d}{d\mu} R_{e^+e^-}(E, \mu, g_s(\mu)) = 0 \quad \longrightarrow \quad \left( \mu \frac{\partial}{\partial \mu} + \beta(g_s) \frac{\partial}{\partial g_s} \right) R_{e^+e^-} = 0, \quad (4)$$

with the beta function

$$\beta(g_s) = \mu \frac{dg_s(\mu)}{d\mu}. \quad (5)$$

Dimensional analysis tells us that the dimensionless ratio  $R_{e^+e^-}$  must be of the form

$$R_{e^+e^-}(E, \mu, g_s(\mu)) = f\left(\frac{E}{\mu}, g_s(\mu)\right). \quad (6)$$

The seemingly uninteresting dependence on  $\mu$  can therefore be traded for the dependence on energy or on the dimensionless ratio  $z = E/\mu$ :

$$\left( -\frac{\partial}{\partial \log z} + \beta(g_s) \frac{\partial}{\partial g_s} \right) f(z, g_s(\mu)) = 0. \quad (7)$$

The general solution of this renormalization group equation is

$$f(z, g_s(\mu)) = \hat{f}(\bar{g}_s(z, g_s)), \quad (8)$$

i.e., a function of a single variable, the energy dependent (running) coupling constant  $\bar{g}_s(z, g_s)$  satisfying

$$\frac{\partial \bar{g}_s}{\partial \log z} = \beta(\bar{g}_s) \quad (9)$$

with the boundary condition  $\bar{g}_s(1, g_s) = g_s$ . For any gauge coupling, the leading one-loop result for the  $\beta$  function is

$$\beta(x) = -\frac{\beta_0}{(4\pi)^2} x^3 \quad (10)$$

implying

$$\bar{g}_s^2(E/\mu, g_s(\mu)) = \frac{g_s^2(\mu)}{1 + \frac{\beta_0}{(4\pi)^2} g_s^2(\mu) \log E^2/\mu^2}. \quad (11)$$

Expanding the denominator, we observe that the renormalization group equation has allowed us to sum the leading logs  $(g_s^2(\mu) \log E^2/\mu^2)^n$  of all orders in perturbation theory. Even more importantly, the energy dependence of the running coupling constant is determined by the sign of  $\beta_0$  in Eq. (10):

$\beta_0 < 0$ :	$\lim_{E \rightarrow 0} \bar{g}(E) = 0$	infrared stable (QED)
$\beta_0 > 0$ :	$\lim_{E \rightarrow \infty} \bar{g}(E) = 0$	ultraviolet stable (QCD)

For the cross section ratio  $R_{e^+e^-}$  we get finally

$$R_{e^+e^-} = R_0 \left( 1 + \frac{g_s^2(E)}{4\pi^2} + O(g_s^4(E)) \right) \quad (12)$$

in terms of  $g_s^2(E) \equiv \overline{g}_s^2(E/\mu, g_s(\mu))$ .

The crucial question in the early seventies was therefore whether QFT was compatible with ultraviolet stability (asymptotic freedom)? The majority view was expressed in a paper by Zee [5]: “... we conjecture that there are no asymptotically free quantum field theories in four dimensions.” While Coleman and Gross set out to prove that conjecture their graduate students Politzer and Wilczek (together with Gross) tried to close a loophole: the  $\beta$  function for nonabelian gauge theories (Yang-Mills theories) was still unpublished and probably unknown to everybody except t’Hooft. In the spring of 1973, the Nobel prize winning work of Politzer and Gross and Wilczek [6] demonstrated that Yang-Mills theories are indeed asymptotically free.

The crucial difference between QED and QCD is that photons are electrically neutral whereas the gluons as carriers of the strong interactions are coloured. Further physical insight can be obtained by taking up an analogy with the electrodynamics of continuous media [7]. Because of Lorentz invariance, the vacuum of a relativistic QFT is characterized by

$$\varepsilon\mu = 1 \quad (13)$$

for the product of permittivity  $\varepsilon$  and permeability  $\mu$ . In QED charge screening implies  $\varepsilon > 1$  so that the vacuum of QED acts like a diamagnet ( $\mu < 1$ ). In QCD the colour charge screening of quarks ( $\varepsilon > 1$ ) is overcompensated by gluons (spin 1) acting as permanent colour dipoles ( $\mu > 1$ ). Because

$$\beta_0^{\text{QCD}} = \frac{1}{3} (11N_c - 2N_F) , \quad (14)$$

the QCD vacuum is a (colour) paramagnet for  $N_F < 11N_c/2 < 17$  quark flavours (for  $N_c = 3$ ). Because of the general relation (13) this can also be interpreted as anti-screening ( $\varepsilon < 1$ ).

The existence of three colours was already widely accepted at that time. Gell-Mann and collaborators had been investigating a model of coloured quarks interacting via a singlet gluon (not asymptotically free). In a contribution of Fritzsch and Gell-Mann in the Proceedings of the High Energy Conference in Chicago in 1972 [8] one finds the probably first reference to nonabelian gluons: “Now the interesting question has been raised lately whether we should regard the gluons as well as the quarks as being non-singlets with respect to colour (J. Wess, private communication to B. Zumino).” Although Gell-Mann is generally credited for the name QCD, the first published occurrence of QCD is much less known (cf., e.g., Refs. [1]). My own investigation of the early literature has produced a footnote in a paper of Fritzsch, Gell-Mann and Minkowski in 1975 [9] suggesting “A good name for this theory is quantum chromodynamics.”

## 1.2 Colour

Already before the arrival of QCD, there were a number of indications for the colour degree of freedom.

### ● Triality problem

In the original quark model often called the naive quark model, the three quarks  $u$ ,  $d$ ,  $s$  give rise to mesonic bound states of the form  $\bar{q}q$ . All of the nine expected bound states had already been observed suggesting an attractive force between all quarks and antiquarks. The baryons fit nicely into  $qqq$  bound states. If the strong force is purely attractive why do antiquarks not bind to baryons? The resulting objects of the form  $\bar{q}qqq$  would have fractional charge and have never been observed. Introducing three colours for each quark and antiquark allows for  $9 \times 9 = 81$  combinations of  $\bar{q}q$  only nine of which had been found. The remaining 72 combinations are not bound states invalidating the previous argument.

### ● Spin-statistics problem

Consider the state

$$|\Delta^{++}(S_z = 3/2)\rangle \sim |u \uparrow u \uparrow u \uparrow\rangle. \quad (15)$$

Since the spin-flavour content is completely symmetric, Fermi statistics for quarks seems to require an antisymmetric spatial wave function. On the other hand, for every reasonable potential the ground state is symmetric in the space variables. Colour solves this problem because the state (15) is totally antisymmetric in the colour indices respecting the generalized Pauli principle with a spatially symmetric wave function.

- Renormalizability of the Standard Model

With the usual charges of quarks and leptons, the Standard Model is a consistent gauge invariant QFT only if there are three species of quarks in order to cancel the so-called gauge anomalies.

- $\pi^0 \rightarrow 2\gamma$  decay

The by far dominant contribution to the decay amplitude is due to the chiral anomaly (exact for massless quarks). The observed rate can only be understood if there are again three species of quarks.

- Momentum balance in deep inelastic scattering

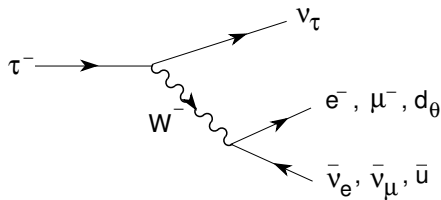
The momentum sum rule indicates that only about 50 % of the nucleon momentum is carried by valence quarks. The remainder is mainly carried by gluons.

- Quark counting

After the advent of QCD, many more direct confirmations of the colour degree of freedom were obtained. One of the first confirmations was provided by the total cross section  $\sigma(e^+ + e^- \rightarrow \text{hadrons})$  already discussed in the previous subsection.

- Hadronic  $\tau$  decays

As we shall discuss in the next lecture, hadronic  $\tau$  decays not only give clear evidence for  $N_c = 3$  but they also provide an excellent opportunity for extracting  $\alpha_s = g_s^2/4\pi$ .



$$\begin{aligned} R_\tau &= \frac{\Gamma(\tau^- \rightarrow \nu_\tau + \text{hadrons})}{\Gamma(\tau^- \rightarrow \nu_\tau e^- \bar{\nu}_e)} \\ &= N_c (|V_{ud}|^2 + |V_{us}|^2) (1 + O(\alpha_s)). \end{aligned} \quad (16)$$

**Fig. 1:** Feynman diagram for  $\tau^- \rightarrow \nu_\tau + X$ .

### 1.3 Gauge invariance

Gauge invariance is a main ingredient not only of QCD but of the Standard Model as a whole. We start with the Lagrangian for a single free Dirac fermion:

$$\mathcal{L}_0 = \bar{\psi}(x) i \not{\partial} \psi(x) - m \bar{\psi}(x) \psi(x), \quad \not{\partial} := \gamma^\mu a_\mu. \quad (17)$$

This Lagrangian and the resulting Dirac equation are invariant under a phase transformation (global  $U(1)$ )

$$\psi(x) \longrightarrow \psi'(x) = e^{-iQ} \psi(x) \quad (18)$$

with  $Q\varepsilon$  an arbitrary real constant. One may now pose the question whether the phase in the transformation law (18) must really be the same here and “behind the moon”, as is the case in (18) with a space-time independent phase  $Q\varepsilon$ . Instead of experimenting behind the moon, we replace the constant  $\varepsilon$  with an arbitrary real function  $\varepsilon(x)$  and see what happens. As is easily checked, the mass term in (17) remains invariant but not the kinetic term because

$$\partial_\mu \psi(x) \longrightarrow e^{-iQ\varepsilon(x)} (\partial_\mu - iQ\partial_\mu \varepsilon(x)) \psi(x) . \quad (19)$$

The conclusion is that the phase must indeed be the same here and behind the moon for the theory to be invariant under transformations of the form (18).

However, there is a well-known procedure for enforcing local invariance, i.e. invariance for a completely arbitrary space-time dependent phase  $\varepsilon(x)$ . We enlarge the theory by introducing a spin-1 vector field  $A_\mu$  that has precisely the right transformation property to cancel the obnoxious piece in (19) with  $\partial_\mu \varepsilon(x)$ . The idea is to replace the ordinary derivative  $\partial_\mu$  by a covariant derivative  $D_\mu$ :

$$D_\mu \psi(x) = (\partial_\mu + iQA_\mu(x)) \psi(x) , \quad (20)$$

with

$$A_\mu(x) \longrightarrow A'_\mu(x) = A_\mu(x) + \partial_\mu \varepsilon(x) . \quad (21)$$

It is easy to check that  $D_\mu \psi$  transforms covariantly,

$$D_\mu \psi(x) \longrightarrow (D_\mu \psi)'(x) = e^{-iQ\varepsilon(x)} D_\mu \psi(x) , \quad (22)$$

so that the enlarged Lagrangian

$$\mathcal{L} = \bar{\psi}(x) (i \not{D} - m) \psi(x) = \mathcal{L}_0 - QA_\mu(x) \bar{\psi}(x) \gamma^\mu \psi(x) \quad (23)$$

is invariant under local  $U(1)$  transformations (gauge invariance).

The most important feature of this exercise is that the requirement of gauge invariance has generated an interaction between the fermion field  $\psi$  and the gauge field  $A_\mu$ . Introducing a kinetic term for the gauge field to promote it to a propagating quantum field, the full Lagrangian

$$\mathcal{L} = \bar{\psi} (i \not{D} - m) \psi - \frac{1}{4} F_{\mu\nu} F^{\mu\nu} \quad (24)$$

is still gauge invariant because the field strength tensor  $F_{\mu\nu} = \partial_\mu A_\nu - \partial_\nu A_\mu$  is automatically gauge invariant. Setting  $Q = -e$  for the electron field, we have “deduced” QED from the free electron theory and the requirement of gauge invariance. For completeness, we take note that a mass term of the form  $M_\gamma^2 A_\mu A^\mu$  is forbidden by gauge invariance implying massless photons.

#### 1.4 $SU(3)_c$ and the QCD Lagrangian

As we have seen, quarks come in three colours. Suppressing all space-time dependence, the free quark Lagrangian for a single flavour has the form

$$\mathcal{L}_0 = \sum_{i=1}^3 \bar{q}_i (i \not{\partial} - m_q) q_i . \quad (25)$$

Assuming the three quarks with different colours to have the same mass  $m_q$  (different flavours have different masses, of course), we can ask for the global invariances of  $\mathcal{L}_0$ . All transformations that leave  $\mathcal{L}_0$  invariant are of the form

$$q_i \longrightarrow q'_i = U_{ij} q_j , \quad U U^\dagger = U^\dagger U = \mathbb{1} \quad (26)$$

with arbitrary unitary matrices  $U_{ij}$ . Splitting off a common phase transformation  $q_i \rightarrow e^{-i\varepsilon} q_i$  treated previously and generating electromagnetic interactions that we know to be colour blind, we are left with the special unitary group  $SU(3)$  comprising all three-dimensional unitary matrices with unit determinant.

In contrast to the  $U(1)$  case treated before, we now have eight independent transformations in  $SU(3)$  (an 8-parameter Lie group). Therefore, continuing in the same spirit as before, it is not just a question of demanding gauge invariance but we also have to find out which part of  $SU(3)$  should be gauged. With hindsight, the following two criteria lead to a unique solution.

- i. The three colours are not like three arbitrary electric charges but are instead intimately connected through gauge transformations. This requires the quarks to be in an irreducible three-dimensional representation leaving only two possibilities: either all of  $SU(3)$  or one of the  $SU(2)$  subgroups must be gauged.
- ii. Quarks and antiquarks transform differently under gauge transformations ( $\underline{3} \neq \underline{3}^*$ ). This closes the case and implies that all  $SU(3)$  transformations must be gauged.

The above requirements guarantee that both  $\bar{q}q$  and  $qqq$  contain colour singlets = hadrons,

$$\underline{3}^* \otimes \underline{3} = \underline{1} \oplus \underline{8}, \quad \underline{3} \otimes \underline{3} \otimes \underline{3} = \underline{1} \oplus \underline{8} \oplus \underline{8} \oplus \underline{10}, \quad (27)$$

but neither  $qq$  nor  $\bar{q}qqq$  or other exotic combinations.

Every three-dimensional unitary matrix with  $\det U = 1$  can be written as

$$U(\varepsilon_a) = \exp\left\{-i \sum_{a=1}^8 \varepsilon_a \frac{\lambda_a}{2}\right\} \quad (28)$$

with eight parameters  $\varepsilon_a$  and with eight traceless hermitian Gell-Mann matrices  $\lambda_a$ . Their commutation relations define the Lie algebra of  $SU(3)$ :

$$[\lambda_a, \lambda_b] = 2i f_{abc} \lambda_c, \quad (29)$$

with real, totally antisymmetric structure constants  $f_{abc}$ .

The gauge principle demands invariance of the theory for arbitrary space-time dependent functions  $\varepsilon_a(x)$ . Instead of a single gauge field  $A_\mu$ , we now need eight vector fields  $G_\mu^a(x)$  entering the covariant derivative

$$(D^\mu q)_i = \left( \partial^\mu \delta_{ij} + i g_s \sum_{a=1}^8 G_\mu^a \frac{\lambda_{a,ij}}{2} \right) q_j =: \{(\partial^\mu + i g_s G^\mu) q\}_i. \quad (30)$$

The real coupling constant  $g_s$  measures the strength of the quark gluon interaction just as the charge  $Q$  is a measure of the electromagnetic interaction. Using the convenient matrix notation (summation convention implied)

$$G_{ij}^\mu := G_\mu^a \frac{\lambda_{a,ij}}{2}, \quad (31)$$

the covariant derivative now transforms as

$$G_\mu \longrightarrow G'_\mu = U(\varepsilon) G_\mu U^\dagger(\varepsilon) + \frac{i}{g_s} (\partial_\mu U(\varepsilon)) U^\dagger(\varepsilon) \quad (32)$$

in order for  $(D_\mu q)_i$  to transform like the  $q_i$  themselves (covariance requirement).



Because of the nonabelian character of  $SU(3)$ , the transformation laws are more complicated than in the electromagnetic case. The differences can already be seen in the infinitesimal transformations of the gluon fields  $G_a^\mu$  following from (32):

$$G_a^\mu \longrightarrow G_a^{\mu'} = G_a^\mu + \frac{1}{g_s} \partial^\mu \varepsilon_a + f_{abc} \varepsilon_b G_c^\mu + O(\varepsilon^2) . \quad (33)$$

In order to have propagating gluon fields, we need an analogue of the electromagnetic field strength tensor  $F_{\mu\nu}$ . The simplest approach is to calculate the commutator of two covariant derivatives:

$$[D_\mu, D_\nu] = [\partial_\mu + i g_s G_\mu, \partial_\nu + i g_s G_\nu] =: i g_s G_{\mu\nu} . \quad (34)$$

The nonabelian field strength tensor  $G^{\mu\nu} = G_a^{\mu\nu} \frac{\lambda_a}{2}$  has the explicit form

$$\begin{aligned} G^{\mu\nu} &= \partial^\mu G^\nu - \partial^\nu G^\mu + i g_s [G^\mu, G^\nu] \\ G_a^{\mu\nu} &= \partial^\mu G_a^\nu - \partial^\nu G_a^\mu - g_s f_{abc} G_b^\mu G_c^\nu \end{aligned} \quad (35)$$

and it transforms covariantly under  $SU(3)$  gauge transformations:

$$G_{\mu\nu} \longrightarrow G'_{\mu\nu} = U(\varepsilon) G_{\mu\nu} U^\dagger(\varepsilon) . \quad (36)$$

The gauge invariant colour trace

$$\text{tr}(G_{\mu\nu} G^{\mu\nu}) = \frac{1}{2} G_a^{\mu\nu} G_{\mu\nu}^a \quad (37)$$

has the right structure for a gluon kinetic term leading immediately to the  $SU(3)_c$  invariant QCD Lagrangian for  $f = 1, \dots, N_F$  quark flavours:

$$\mathcal{L}_{\text{QCD}} = -\frac{1}{2} \text{tr}(G_{\mu\nu} G^{\mu\nu}) + \sum_{f=1}^{N_F} \bar{q}_f (i \not{D} - m_f \mathbb{1}_c) q_f . \quad (38)$$

As in the  $U(1)$  case, gauge invariance requires massless gluons. Writing out the Lagrangian (38) in detail, one finds three types of vertices instead of a single one for QED:

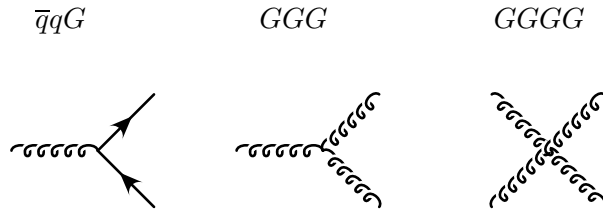


**Fig. 2:** Basic vertices of QCD.

In addition to the quark masses, QCD has a single parameter describing the strength of the strong interactions, the strong coupling constant  $g_s$  ( $\alpha_s = g_s^2/4\pi$ ).

Experimental group theory

Can experimentalists determine more than a single coupling strength  $\alpha_s$  in a strong process? All the information is contained in the vertices: in addition to  $g_s$ , the vertices also contain the two matrices

$$(t_a^F)_{ij} = \frac{1}{2} (\lambda_a)_{ij} , \quad (t_a^A)_{bc} = -i f_{abc} , \quad (39)$$

defining the fundamental and adjoint representations of (the Lie algebra of)  $SU(3)$ :

$$[t_a, t_b] = i f_{abc} t_c . \quad (40)$$

Let us pretend for a moment that we don't know that there are three colours and eight gluons. For a general (compact Lie) group of symmetry transformations, the vertices are again determined by quark and gluon representation matrices  $t_a^F, t_a^A$ . The combinations that actually appear in measurable quantities are the following traces and sums:

$$\text{tr}(t_a^R t_b^R) = T_R \delta_{ab}, \quad \sum_a (t_a^R)_{ij} (t_a^R)_{jk} = C_R \delta_{ik} \quad (R = F, A) , \quad (41)$$

with

$$\begin{aligned} T_R: & \quad \text{Dynkin index for the representation R;} \\ C_R: & \quad \text{(quadratic) Casimir for R.} \end{aligned}$$

For a  $d_R$ -dimensional representation, one derives from the definitions (41) the general relation

$$d_R C_R = n_G T_R \quad (42)$$

where  $n_G$  is the number of independent parameters of  $G$ . Restricting the discussion to  $SU(n)$ , the two cases of interest are

$R = A$  (adjoint representation):

$$d_A = n_G \quad \longrightarrow \quad C_A = T_A = n \quad \text{for } SU(n);$$

$R = F$  (fundamental representation of  $SU(n)$ ):

$$d_F = n, \quad n_G = n^2 - 1, \quad T_F = 1/2 \quad \longrightarrow \quad C_F = \frac{n^2 - 1}{2n}$$

and for the special case of  $SU(3)$ :  $C_F = \frac{4}{3}, C_A = T_A = N_c = 3$ .

The independent quantities that can be measured are  $C_F$  and  $C_A$ . A combined jet analysis in  $e^+e^-$  annihilation at LEP found [10]

$$C_F = 1.30 \pm 0.01(\text{stat}) \pm 0.09(\text{sys}), \quad C_A = 2.89 \pm 0.03(\text{stat}) \pm 0.21(\text{sys}) \quad (43)$$

in manifest agreement with  $SU(3)$ .

Feynman diagrams are constructed with the vertices and propagators of the QCD Lagrangian (38). The problem here is the same as in QED: due to the gauge invariance of (38), the gluon propagator does not exist. At least for perturbation theory, the inescapable consequence is that gauge invariance must be broken in the Lagrangian! Or, in a more euphemistic manner of speaking, the gauge must be fixed. In the simplest and widely used version (covariant gauge with real parameter  $\xi$ ) the Lagrangian (38) is replaced by

$$\mathcal{L}_{\text{QCD}} \quad \longrightarrow \quad \mathcal{L}_{\text{QCD}} - \frac{\xi}{2} (\partial_\mu G_a^\mu)^2 + \mathcal{L}_{\text{ghost}} . \quad (44)$$

The gluon propagator now exists ( $\xi = 1$ : Feynman gauge):

$$\Delta_{ab}^{\mu\nu}(k) = \delta_{ab} \frac{-i}{k^2 + i\epsilon} \left( g^{\mu\nu} + (\xi^{-1} - 1) \frac{k^\mu k^\nu}{k^2} \right) \stackrel{\xi=1}{=} \delta_{ab} \frac{-i g^{\mu\nu}}{k^2 + i\epsilon} . \quad (45)$$

The additional ghost Lagrangian  $\mathcal{L}_{\text{ghost}}$  repairs the damage done by gauge fixing: although Green functions are now gauge dependent, observable S-matrix elements are still gauge invariant and therefore independent of  $\xi$  (Feynman, Faddeev, Popov, BRST, ...).

## 2 Perturbative QCD

### 2.1 QCD at tree level

The calculation of tree amplitudes in QCD is straightforward but

- to compare theory with experiment, we must have hadrons rather than quarks and gluons in the initial and final states;
- amplitudes and cross sections are in general infrared divergent for massless gluons.

The general recipe is to consider infrared safe quantities, the more inclusive the better. A good example is once more  $e^+e^- \rightarrow \text{hadrons}$ .

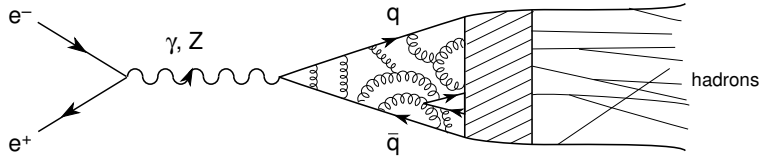


**Fig. 3:**  $e^+e^- \rightarrow \text{hadrons}$ .

The sum over all hadronic final states can be expressed in terms of the imaginary (absorptive) part of the two-point function of electromagnetic currents (photonic case), the hadronic vacuum polarization:

$$\Pi_{\text{em}}^{\mu\nu}(q) = i \int d^4x e^{iq \cdot x} \langle 0 | T J_{\text{em}}^\mu(x) J_{\text{em}}^\nu(0) | 0 \rangle = (-g^{\mu\nu} q^2 + q^\mu q^\nu) \Pi_{\text{em}}(q^2). \quad (46)$$

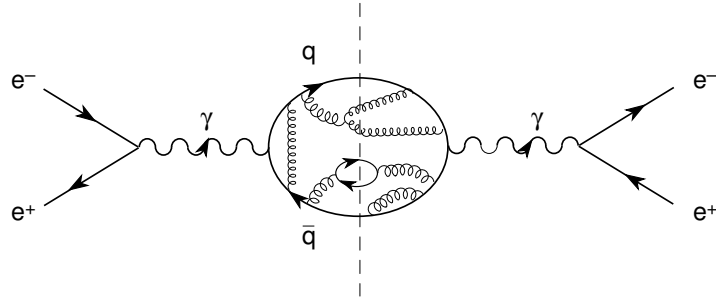


**Fig. 4:** Hadronic vacuum polarization.

The sum over all intermediate states can be performed either with quarks and gluons or with hadrons. Since there are no massless hadrons, the hadronic vacuum polarization is infrared safe.

To lowest order in QCD, the amplitude for

$$e^+e^- \rightarrow \gamma^*(Z^*) \rightarrow \bar{q}q \quad (47)$$

is in fact independent of the strong coupling constant  $g_s$ . Except for the charges, masses and multiplicities of quarks, it is the same calculation as for  $e^+e^- \rightarrow \mu^+\mu^-$  in QED. Therefore, for quarks with given flavour  $f$  and colour  $i$  the amplitude is (neglecting  $m_e, m_\mu, m_q$ )

$$A(e^+e^- \rightarrow \bar{q}_f^i q_f^i) = \frac{Q_f}{e} A(e^+e^- \rightarrow \mu^+\mu^-). \quad (48)$$

Quarks and antiquarks with different colour and flavour are in principle distinguishable so that the total hadronic cross section, normalized to  $\sigma(e^+e^- \rightarrow \mu^+\mu^-)$ , is

$$R_{e^+e^-} = \frac{\sigma(e^+e^- \rightarrow \text{hadrons})}{\sigma(e^+e^- \rightarrow \mu^+\mu^-)} = \sum_{i,f} Q_f^2/e^2 = N_c \sum_f Q_f^2/e^2. \quad (49)$$

As shown in Fig. 5, this is a good approximation to the experimental data between quark thresholds.

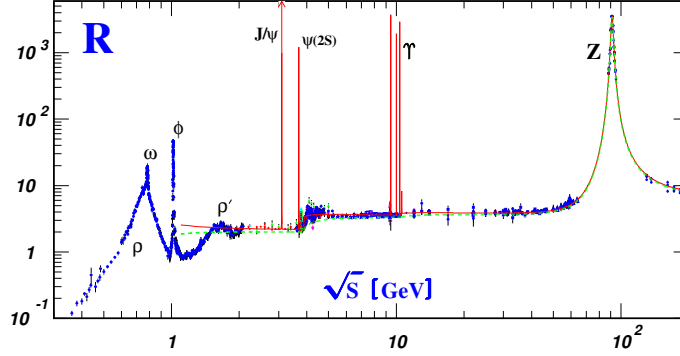


**Fig. 5:** Experimental data for  $R_{e^+e^-}$  taken from Ref. [11].

A similar result is obtained for the hadronic width of the  $Z$ :

$$R_Z = \Gamma(Z \rightarrow \text{hadrons})/\Gamma(Z \rightarrow e^+e^-) = N_c(1 + \delta_{\text{EW}}) \sum_f (v_f^2 + a_f^2)/(v_e^2 + a_e^2), \quad (50)$$

where  $v_F, a_F$  are the (axial-)vector couplings for  $Z \rightarrow \bar{F}F$ .

$e^+ e^- \rightarrow \text{jets}$

At high energies, the two-jet structure from  $e^+e^- \rightarrow \bar{q}q$  dominates, being the only process at  $O(\alpha_s^0)$ . At  $O(\alpha_s)$  and omitting  $Z$  exchange, we have in addition gluon bremsstrahlung off quarks giving rise to a three-jet structure:

$$e^+(q_1)e^-(q_2) \rightarrow q(p_1)\bar{q}(p_2)G(p_3). \quad (51)$$

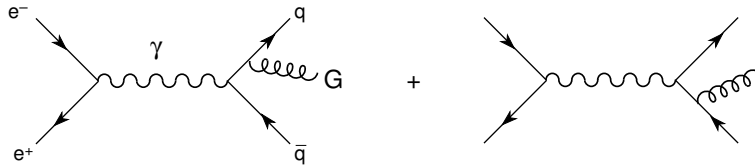


**Fig. 6:** Leading-order diagrams for three-jet production.

The calculation is again identical to QED bremsstrahlung except for a factor (sum over all final states in the rate)

$$\sum_a \text{tr}(t_a^F t_a^F) = T_F \sum_a \delta_{aa} = T_F n_{SU(3)} = d_F C_F = 3 C_F = 4. \quad (52)$$

With the kinematics specified by

$$\begin{aligned} s &= (q_1 + q_2)^2, & (p_i + p_j)^2 &= (q_1 + q_2 - p_k)^2 =: s(1 - x_k) \\ x_1 + x_2 + x_3 &= 2, & \text{CMS : } x_i &= 2E_i/\sqrt{s}, \end{aligned} \quad (53)$$

the double differential cross section (for massless quarks) is found to be

$$\frac{d^2\sigma}{dx_1 dx_2} = \frac{2\alpha_s\sigma_0}{3\pi} \frac{x_1^2 + x_2^2}{(1-x_1)(1-x_2)} \quad \text{with} \quad \sigma_0 = \frac{4\pi\alpha^2}{s} \sum_f (Q_f/e)^2. \quad (54)$$

The problem with this cross section is that it diverges for  $x_i \rightarrow 1$  ( $i = 1, 2$ ). This infrared divergence is due the singular behaviour of the quark propagator and it happens even for massive quarks:

$$(p_2 + p_3)^2 - m_q^2 = 2p_2 \cdot p_3 = s(1 - x_1). \quad (55)$$

$m_q > 0$  :  $x_1 \rightarrow 1$  only possible for  $p_3 \rightarrow 0$  (soft gluon singularity);

$m_q = 0$  :  $x_1 = 1$  also possible for  $p_3 \parallel p_2$  (collinear singularity) .

To understand the origin of infrared divergences, we first take the viewpoint of an experimentalist measuring three-jet events where the jets stand for the quarks and the gluon in the final state.

- Depending on the detector resolution, a quark and a soft gluon cannot be distinguished from a single quark. In that case, the event will be counted as a two-jet event.
- Two collinear massless particles can never be resolved: they always stay together.

From the viewpoint of a theorist, we recall that perturbation theory is built on the assumption that particles do not interact when they are sufficiently far apart. This assumption is not really satisfied for massless quanta like photons or gluons that give rise to long-range forces. In other words, an electron (a quark) can never be separated from its cloud of soft photons (gluons).

The practitioner's solution of the infrared problem is well understood:

- One must define criteria to distinguish between (in the present case) two- and three-jet events (jet algorithms).
- Virtual gluon (loop) corrections for the process  $e^+e^- \rightarrow \bar{q}q$  must be included.

## 2.2 Higher-order corrections and renormalization

The loop corrections of  $O(\alpha_s)$  for  $e^+e^- \rightarrow \bar{q}q$  are calculated from the Feynman diagrams below.

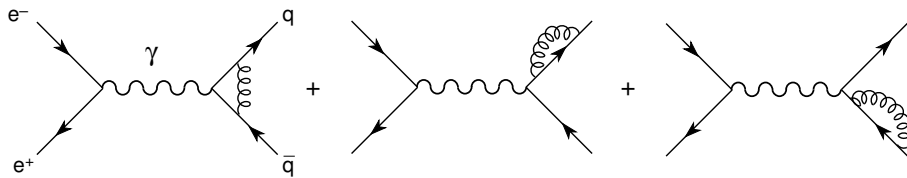


**Fig. 7:** One-loop diagrams for  $e^+e^- \rightarrow \bar{q}q$ .

The resulting amplitudes are both infrared and ultraviolet divergent.

In contrast to infrared divergences, ultraviolet divergences are due to the high-momentum components of the particles in loops. Common sense tells us that those components cannot influence physics at

low energies. If this were the case we would have to give up all hopes of being able to make predictions at presently accessible energies.

The recipe to handle ultraviolet divergences is also well understood. One first has to choose a method to cut off the high-momentum components. There are infinitely many ways to do that so the question is legitimate whether the final amplitudes will depend on that procedure rendering the result completely arbitrary. The answer is that the cutoff procedure (regularization) must always be accompanied by renormalization. Before choosing a suitable regularization procedure let us therefore try to understand the idea of renormalization, using the most naive regularization method.

To simplify matters as much as possible, we consider the elastic scattering of two particles in massless scalar  $\phi^4$  theory ( $\mathcal{L}_{\text{int}} \sim \lambda\phi^4$ ):

$$\phi\phi \rightarrow \phi\phi, \quad (56)$$

with scattering amplitude  $A(s, t)$  in terms of the usual Mandelstam variables. We now define what we mean by the physical (renormalized) coupling constant. The definition should be applicable at every order of perturbation theory and it should coincide with the constant  $\lambda$  in the Lagrangian at tree level. A possible definition in scalar  $\phi^4$  theory is

$$\lambda_r(\mu) := A(s = -t = \mu^2) \quad (57)$$

with an arbitrary renormalization scale  $\mu$ . At tree level,  $A(s, t)$  is momentum independent and with the proper normalization we have indeed  $\lambda_r(\mu) = \lambda$ .

Beyond tree level, the amplitude has an ultraviolet divergence that we regularize with a simple momentum cutoff  $\Lambda$  here. The relevant diagrams up to one loop are shown in Fig. 8.

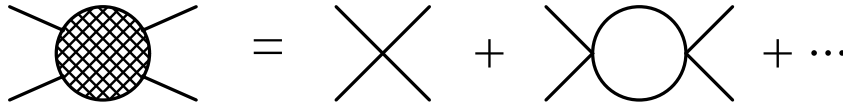


**Fig. 8:** Scattering amplitude for  $\phi\phi \rightarrow \phi\phi$  to one-loop order.

Setting  $s = -t = \mu^2$ , one finds ( $\beta_0$  is a constant)

$$\begin{aligned} \lambda_r(\mu) = A(s = -t = \mu^2) &= \lambda + \beta_0 \lambda^2 \log \Lambda / \mu \\ &+ \mu\text{-independent terms of } O(\lambda^2) + O(\lambda^3). \end{aligned} \quad (58)$$

Since  $\lambda_r(\mu)$  is finite, being equal to the physical scattering amplitude at some fixed point in phase space, the bare coupling  $\lambda$  diverges as the cutoff  $\Lambda \rightarrow \infty$ . However, the bare coupling is not related to any physical quantity. Therefore, we are free to “sweep the infinities under the rug” as long as this is done in a transparent and controllable way.

To do this, we change the renormalization scale by a small amount  $\delta\mu$ :

$$\begin{aligned} \lambda_r(\mu + \delta\mu) - \lambda_r(\mu) &= \beta_0 \lambda^2 \log \left( \frac{\Lambda}{\mu + \delta\mu} \frac{\mu}{\Lambda} \right) + O(\lambda^3) \\ &= \beta_0 \lambda_r^2 \log \frac{\mu}{\mu + \delta\mu} + O(\lambda_r^3) = -\beta_0 \lambda_r^2 \frac{\delta\mu}{\mu} + O[(\delta\mu)^2] + O(\lambda_r^3). \end{aligned} \quad (59)$$

The bare coupling and the cutoff have disappeared in the last equation. Expanding  $\lambda_r(\mu + \delta\mu)$  around  $\mu$  and letting  $\delta\mu \rightarrow 0$ , we recover the  $\beta$  function of  $\phi^4$  theory to one-loop order:

$$\mu \frac{d\lambda_r(\mu)}{d\mu} = -\beta_0 \lambda_r^2(\mu) + O(\lambda_r^3) = \beta(\lambda_r(\mu)). \quad (60)$$

Unlike in Yang-Mills theories,  $\beta_0 < 0$  so that  $\phi^4$  theory is ultraviolet unstable like all quantum field theories except nonabelian gauge theories [5, 12]. However, for understanding the essence of renormalization the important observation is that physical quantities do not depend on the bare coupling constant  $\lambda$  nor on the cutoff  $\Lambda$  (for  $\Lambda \rightarrow \infty$ ) but only on the renormalized coupling  $\lambda_r(\mu)$ . For the purpose of comparing theory with experiment at present energies, we will never notice the stuff that was swept under the rug.

We now turn to the choice of a regularization scheme. Although there are infinitely many possibilities, some choices are clearly better than others. The main criteria are:

- ☛ The regularization method should respect symmetries of the theory as much as possible. In this respect, the previously employed momentum cutoff is as bad as it gets violating Poincaré symmetry, gauge invariance, etc.
- ☛ The scheme should violate only those symmetries that are necessarily violated by quantum effects (anomalies).
- ☛ The method should be simple to handle in practice.

From the practitioner's point of view, dimensional regularization is the almost unique choice fulfilling these criteria. Let us demonstrate the method with a simple example, electronic vacuum polarization (setting  $m_e = 0$ ).

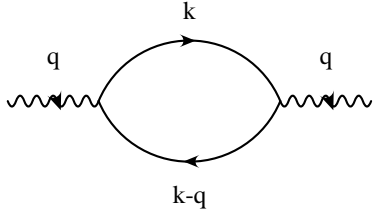


**Fig. 9:** Vacuum polarization at one loop.

Gauge invariance, guaranteed by dim. regularization, implies the same structure as in the hadronic case:

$$\Pi^{\mu\nu}(q) = (-g^{\mu\nu}q^2 + q^\mu q^\nu) \Pi(q^2) \quad (61)$$

$$\Pi(q^2) = \frac{8e^2\Gamma(\varepsilon)}{(4\pi)^{2-\varepsilon}} \int_0^1 \frac{dx x(1-x)}{[-q^2x(1-x)]^\varepsilon}$$

$$\Gamma(x) = 1/x - \gamma + O(x), \quad 2\varepsilon = 4 - d.$$

Since dimensional regularization works in  $d$  dimensions, there is a small problem here: there is no scale for  $\log(-q^2)$  that will appear in the explicit form of  $\Pi(q^2)$ . To solve the problem, we insert unity (the scale  $\mu$  and the constant  $c$  are completely arbitrary) in the expression and expand the second factor in  $\varepsilon$ :

$$1 = (c\mu)^{-2\varepsilon} (c\mu)^{2\varepsilon} = (c\mu)^{-2\varepsilon} [1 + \varepsilon \log \mu^2 + 2\varepsilon \log c + O(\varepsilon^2)] . \quad (62)$$

Various schemes on the market differ by the constant  $c$ :

$\overline{\text{MS}}$	$c = 1$
$\overline{\text{MS}}$	$\log c = (\gamma - \log 4\pi)/2$ .

Using the most popular scheme ( $\overline{\text{MS}}$ ), the final result is

$$\begin{aligned} \Pi(q^2) &= \frac{e^2}{12\pi^2} \left\{ \frac{(c\mu)^{-2\varepsilon}}{\varepsilon} - \log(-q^2/\mu^2) + \frac{5}{3} \right\} + O(\varepsilon) \\ &= \Pi_{\text{div}}^{\overline{\text{MS}}}(\varepsilon, \mu) - \frac{e^2}{12\pi^2} \left\{ \log(-q^2/\mu^2) - \frac{5}{3} \right\} . \end{aligned} \quad (63)$$

The divergent part  $\Pi_{\text{div}}^{\overline{\text{MS}}}(\varepsilon, \mu)$  has been isolated and it will be absorbed by wave function renormalization of the photon field contributing to charge renormalization. We also notice that the coefficients of  $1/\varepsilon$  and  $-\log(-q^2/\mu^2)$  are identical: the  $\beta$  function can be extracted from the divergent part. The stuff under the rug is useful after all.

Back to the loop corrections of Fig. 7, we observe that the diagrams give rise to an amplitude proportional to  $g_s^2$ , whereas  $A(e^+e^- \rightarrow \bar{q}qG) \sim g_s$ . How can the infrared divergences cancel among amplitudes of different order in  $g_s$ ? The answer is that they cannot cancel on the level of amplitudes because the final states are different. Not the amplitudes but the rates must be added. Interference with the tree amplitude produces an  $O(\alpha_s)$  term in  $\sigma(e^+e^- \rightarrow \bar{q}q)$  that can and will cancel the infrared divergence in  $\sigma(e^+e^- \rightarrow \bar{q}qG)$ . For details of the calculation I refer to the monograph [13], an excellent source for applications of perturbative QCD in general.

The easier part are the loop corrections for  $\sigma(e^+e^- \rightarrow \bar{q}q)$ . With dimensional regularization to regularize the infrared divergences, one finds

$$\sigma_{\bar{q}q}^{\text{interference}} = \sigma_0 C_F \frac{\alpha_s}{4\pi} H(\varepsilon) \left\{ -\frac{4}{\varepsilon^2} - \frac{6}{\varepsilon} - 16 + O(\varepsilon) \right\}, \quad H(0) = 1. \quad (64)$$

The less familiar part is the three-body phase space integration in  $d$  dimensions giving rise to

$$\sigma_{\bar{q}qG} = \sigma_0 C_F \frac{\alpha_s}{4\pi} H(\varepsilon) \left\{ \frac{4}{\varepsilon^2} + \frac{6}{\varepsilon} + 19 + O(\varepsilon) \right\}. \quad (65)$$

The infrared divergences cancel as expected.

Adding the lowest-order cross section, one obtains finally

$$\sigma(e^+e^- \rightarrow \text{hadrons}) = \sigma_0 \left( 1 + 3C_F \frac{\alpha_s}{4\pi} + O(\alpha_s^2) \right) = \sigma_0 \left( 1 + \frac{\alpha_s}{\pi} + O(\alpha_s^2) \right), \quad (66)$$

with  $\sigma_0$  defined in Eq. (54). The cross section  $\sigma(e^+e^- \rightarrow \text{hadrons})$  is nowadays known up to  $O(\alpha_s^3)$ . Replacing  $\alpha_s$  by the renormalization group improved running coupling  $\alpha_s(\sqrt{s})$ , the general result for  $R_{e^+e^-}$  can be written

$$\begin{aligned} R_{e^+e^-}(s) &= N_c \sum_f Q_f^2/e^2 \left\{ 1 + \sum_{n \geq 1} C_n \left( \frac{\alpha_s(\sqrt{s})}{\pi} \right)^n \right\} \\ &= R_{e^+e^-}^{(0)} \left\{ 1 + C_1 \frac{\alpha_s(\mu)}{\pi} + \left[ C_2 - C_1 \frac{\beta_0}{4} \log(s/\mu^2) \right] \left( \frac{\alpha_s(\mu)}{\pi} \right)^2 + \dots \right\}. \end{aligned} \quad (67)$$

The normalization is such that  $C_1 = 1$ , the coefficients  $C_2, C_3$  being also known.

In principle,  $R_{e^+e^-}(s)$  is independent of the arbitrary scale  $\mu$  by construction. In reality, the unavoidable truncation of the perturbative series introduces a scale dependence. Although there is no unique prescription for the optimal choice of  $\mu$ , the obvious choice here is  $\mu^2 = s$  to avoid large logarithms. If the perturbative expansion is to make sense, we expect higher orders to mitigate the scale dependence. This is nicely demonstrated in Fig. 10 taken from Ref. [13] where the deviation (in percent) of  $R_{e^+e^-}(\sqrt{s} = 33 \text{ GeV})$  from  $R_{e^+e^-}^{(0)}$  is plotted as a function of  $\mu$ . As expected,  $\mu^2 = s$  is indeed a very reasonable choice already at  $O(\alpha_s)$  (L).



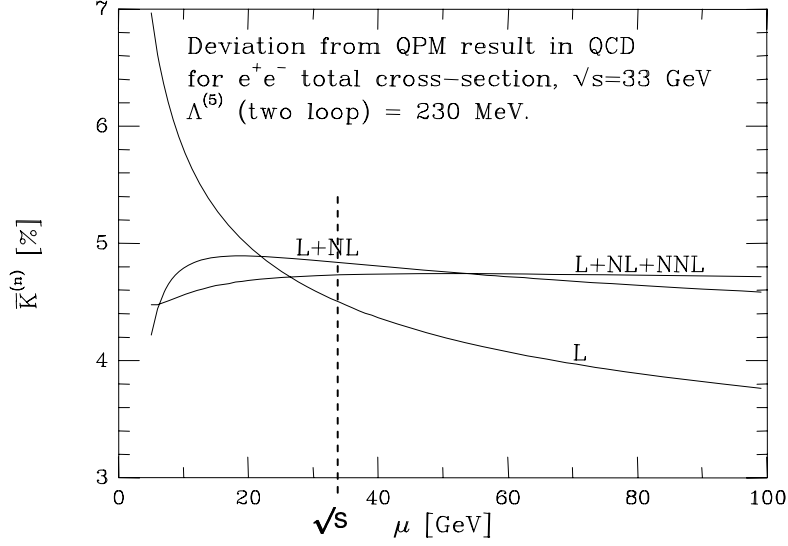


**Fig. 10:** Improvement of the scale dependence in higher orders of perturbation theory for  $R_{e^+e^-}$  ( $\sqrt{s} = 33$  GeV) (taken from the book of Ellis, Stirling and Webber [13]).

### 2.3 Measurements of $\alpha_s$

How should one characterize the coupling strength of QCD? After all, the scale  $\mu$  is arbitrary and, in addition,  $\alpha_s(\mu)$  is in general scheme dependent. For qualitative purposes, one may introduce a scale  $\Lambda_{\text{QCD}}$  that is independent of the renormalization scale  $\mu$ . The drawback is that this quantity is scheme independent only at leading (one-loop) order:

$$\alpha_s(E) = \frac{4\pi}{\beta_0 \log(E^2/\Lambda_{\text{QCD}}^2)}. \quad (68)$$

The coefficient  $\beta_0$  is defined by rewriting the  $\beta$  function for  $\alpha_s$  (instead for  $g_s$  as in Sec. 1.1):

$$\mu \frac{d\alpha_s(\mu)}{d\mu} = 2\beta(\alpha_s) = -\frac{\beta_0}{2\pi} \alpha_s^2 - \frac{\beta_1}{4\pi^2} \alpha_s^3 + \dots \quad (69)$$

The  $\beta$  function is known up to four loops (coefficient  $\beta_3$ ) but only the first two coefficients

$$\beta_0 = 11 - 2N_F/3, \quad \beta_1 = 51 - 19N_F/3 \quad (70)$$

are scheme and gauge independent.

Since the scheme dependence is unavoidable, the coupling strength is nowadays usually given in the form of  $\alpha_s^{\overline{\text{MS}}}(M_Z)$ . Of course, this fixes  $\alpha_s^{\overline{\text{MS}}}(\mu)$  at any scale via the integral

$$\log(\mu_2^2/\mu_1^2) = \int_{\alpha_s(\mu_1)}^{\alpha_s(\mu_2)} \frac{dx}{\beta(x)}. \quad (71)$$

To get a first rough estimate of  $\alpha_s$ , consider the leading-order prediction

$$R_{e^+e^-}(M_Z) = R_{e^+e^-}^{(0)}(M_Z) \left( 1 + \frac{\alpha_s(M_Z)}{\pi} \right). \quad (72)$$

Comparing the combined LEP result [14]  $R_{e^+e^-}(M_Z) = 20.767 \pm 0.025$  with the tree-level prediction  $R_{e^+e^-}^{(0)}(M_Z) = 19.984$ , one obtains

$$\alpha_s(M_Z) = 0.123 \pm 0.004, \quad (73)$$

close to the full three-loop result and not bad at all for a first estimate. A compilation of results can be found in the Review of Particle Properties [14]. In Figs. 11 and 12, the most recent data compiled by Bethke [15] are shown.

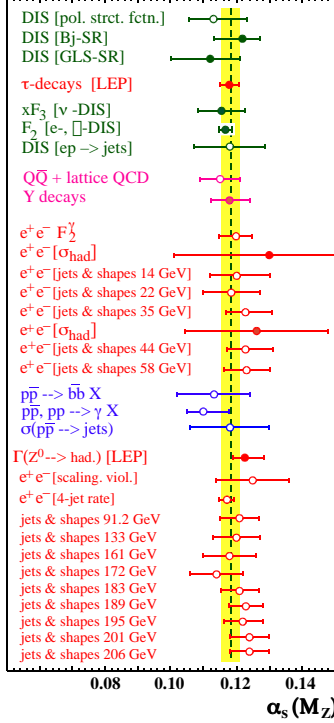


**Fig. 11:** Compilation of data for the extraction of  $\alpha_s^{\overline{\text{MS}}}(M_Z)$  by Bethke [15].

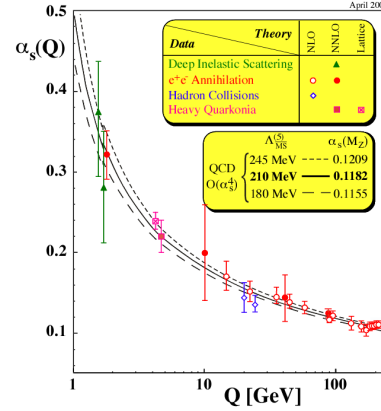


**Fig. 12:** Energy dependence of the running coupling constant  $\alpha_s^{\overline{\text{MS}}}(Q)$  [15].

The first impression is the remarkable agreement among experiments and with theory. However, for determining the best value of  $\alpha_s(M_Z)$ , the following two problems must be kept in mind:

- Different observables are known with different theoretical accuracy: next-to-leading order (NLO) vs. next-to-next-to-leading order (NNLO). Not only the scale dependence but also different scheme dependences must be taken into account.
- Theoretical errors are not normally distributed.

Using only NNLO results, Bethke found [15]

$$\alpha_s(M_Z) = 0.1182 \pm 0.0027, \quad (74)$$

very similar to the PDG average [14] (using a different procedure)

$$\alpha_s(M_Z) = 0.1187 \pm 0.0020. \quad (75)$$

All values in this paragraph refer to  $\alpha_s^{\overline{\text{MS}}}(M_Z)$ .

## 2.4 Hadronic $\tau$ decays

A remarkably precise value for  $\alpha_s^{\overline{\text{MS}}}(M_Z)$  comes from hadronic  $\tau$  decays. At first sight, this is quite surprising because at the natural scale  $\mu = m_\tau$  one has approximately  $\alpha_s(m_\tau) \simeq 0.35$ . Can one expect reasonable convergence of the perturbative series for such a large coupling and how big are the nonperturbative corrections?

The first systematic investigation of  $R_\tau = \Gamma(\tau^- \rightarrow \nu_\tau + \text{hadrons})/\Gamma(\tau^- \rightarrow \nu_\tau e^- \bar{\nu}_e)$  was performed by Braaten, Narison and Pich [16]. The analysis is similar to the one for  $R_{e^+e^-}$ , with obvious modifications: the electromagnetic current (coupling to  $e^+e^-$ ) must be replaced by the charged weak current (coupling to  $\tau\nu_\tau$ ).

We start again with the two-point function (of weak currents  $L^\mu = \bar{u}\gamma^\mu(1 - \gamma_5)d_\theta$ ):

$$\begin{aligned}\Pi_L^{\mu\nu}(q) &= i \int d^4x e^{iq \cdot x} \langle 0 | T L^\mu(x) L^\nu(0)^\dagger | 0 \rangle \\ &= (-g^{\mu\nu} q^2 + q^\mu q^\nu) \Pi_L^{(1)}(q^2) + q^\mu q^\nu \Pi_L^{(0)}(q^2),\end{aligned}\quad (76)$$

with  $d_\theta$  the Cabibbo rotated  $d$ -quark field. One major difference to the electromagnetic case is that one has to integrate over the neutrino energy or, equivalently, over the hadronic invariant mass  $s$ :

$$R_\tau = 12\pi \int_0^{m_\tau^2} \frac{ds}{m_\tau^2} \left(1 - \frac{s}{m_\tau^2}\right)^2 \left\{ \left(1 + 2\frac{s}{m_\tau^2}\right) \text{Im}\Pi_L^{(1)}(s) + \text{Im}\Pi_L^{(0)}(s) \right\}. \quad (77)$$

The problem is that the integration extends all the way down to  $s = 0$  (for  $m_u = m_d = 0$ ) where perturbation theory is certainly not applicable.

However, QFT provides information about the analytic structure of two-point functions that can be used in a standard manner to circumvent the problem. The invariant functions  $\Pi_L^{(0,1)}(s)$  are known to be analytic in the complex  $s$ -plane with a cut on the positive real axis. Therefore, Cauchy's theorem tells us that the contour integral in Fig. 13 vanishes.

One can now trade the integral along the cut of

$$\text{Im}\Pi_L^{(0,1)}(s) = \frac{1}{2i} \left[ \Pi_L^{(0,1)}(s + i\varepsilon) - \Pi_L^{(0,1)}(s - i\varepsilon) \right] \quad (78)$$

for an integral along the circle  $|s| = m_\tau^2$  in the complex  $s$ -plane. It turns out that the nonperturbative corrections are now manageable, being suppressed as  $(\Lambda_{\text{QCD}}/m_\tau)^6$ . Very helpful in this respect is the factor  $\left(1 - \frac{s}{m_\tau^2}\right)^2$  in the integrand that suppresses potentially big contributions near the endpoint of the cut.

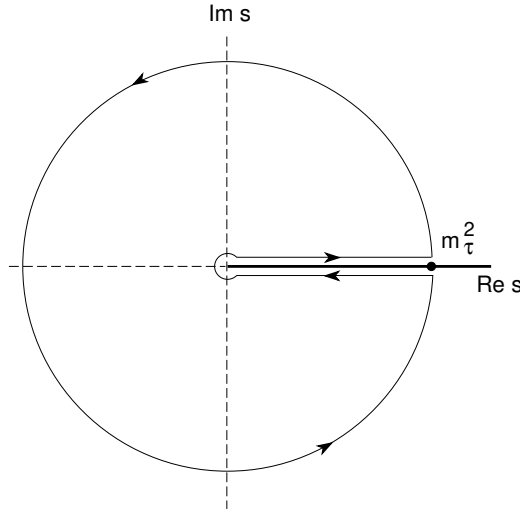


**Fig. 13:** Contour in the complex  $s$ -plane for the two-point functions  $\Pi_L^{(0,1)}(s)$ .

The final result can be written in the form [16]

$$R_\tau = 3 (|V_{ud}|^2 + |V_{us}|^2) S_{EW} \{1 + \delta'_{EW} + \delta_{\text{pert}} + \delta_{\text{nonpert}}\} \quad (79)$$

with leading and nonleading electroweak corrections  $S_{EW} = 1.0194$  and  $\delta'_{EW} = 0.0010$ , respectively. The perturbative QCD corrections of interest for the extraction of  $\alpha_s$  are contained in

$$\begin{aligned} \delta_{\text{pert}} &= \frac{\alpha_s(m_\tau)}{\pi} + \left(C_2 + \frac{19}{48}\beta_0\right) \left(\frac{\alpha_s(m_\tau)}{\pi}\right)^2 + \dots \\ &= \frac{\alpha_s(m_\tau)}{\pi} + 5.2 \left(\frac{\alpha_s(m_\tau)}{\pi}\right)^2 + 26.4 \left(\frac{\alpha_s(m_\tau)}{\pi}\right)^3 + O(\alpha_s(m_\tau)^4). \end{aligned} \quad (80)$$

Finally, the best estimates of nonperturbative contributions, using QCD sum rules and experimental input, yield

$$\delta_{\text{nonpert}} = -0.014 \pm 0.005. \quad (81)$$

From the PDG fit for  $R_\tau$  one then obtains  $\alpha_s(m_\tau) = 0.35 \pm 0.03$ . More interestingly, running this value down to  $M_Z$  with the help of the four-loop  $\beta$  function, one finds

$$\alpha_s(M_Z) = 0.121 \pm 0.0007(\text{exp}) \pm 0.003(\text{th}), \quad (82)$$

not only compatible but in fact very much competitive with other high-precision determinations.

## 2.5 Deep inelastic scattering

From the conception of QCD till today, deep inelastic scattering of leptons on hadrons has had an enormous impact on the field. It is also a classic example for the factorization between long- and short-distance contributions.

Let us start with the kinematics of (in)elastic electron-proton scattering  $e^-(k) + p(p) \rightarrow e^-(k') + X(p_X)$  shown in Fig. 14. In the case of elastic scattering ( $X = p$ ), we have

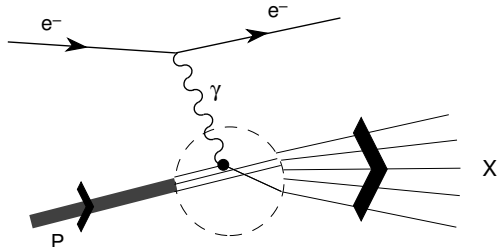
$$W^2 = m^2, \quad Q^2 = 2m\nu, \quad x = 1 \quad (83)$$

and the usual two variables are  $s = (p + k)^2$ ,  $Q^2$  with the differential cross section  $d\sigma(s, Q^2)/dQ^2$ .

For the inclusive scattering, there is a third independent variable: a convenient choice is  $s, x, y$  with  $0 \leq x \leq 1$ ,  $0 \leq y \leq 1$ . In general, we distinguish different types of deep inelastic scattering:

type	exchange
neutral current (NC) DIS	$\gamma, Z, \gamma Z$ -interference
charged current (CC) DIS	$W^\pm$

For these lectures, I will restrict the discussion to photon exchange and to unpolarized (spin-averaged) DIS.



$$\begin{aligned} q &= k - k', \quad Q^2 = -q^2 > 0, \quad p^2 = m^2 \\ \nu &= p \cdot q / m = E - E' \quad (\text{target rest frame}) \\ x &= \frac{Q^2}{2m\nu}, \quad y = \frac{p \cdot q}{p \cdot k} = 1 - E'/E \\ W^2 &= p_X^2 = (p + q)^2 = m^2 + 2m\nu - Q^2 \geq m^2. \end{aligned}$$

Fig. 14: Deep inelastic scattering.

The matrix element for the diagram in Fig. 14 has the structure  $e l(\text{epton})_\mu \frac{g^{\mu\nu}}{Q^2} e h(\text{adron})_\nu$ , with leptonic and hadronic current matrix elements  $l(\text{epton})_\mu$  and  $h(\text{adron})_\nu$ , respectively. The resulting double differential cross section is of the form

$$\begin{aligned} \frac{d^2\sigma}{dx dy} &= x(s - m^2) \frac{d^2\sigma}{dx dQ^2} = \frac{2\pi y \alpha^2}{Q^4} L_{\mu\nu} H^{\mu\nu} \\ L_{\mu\nu} &= 2(k_\mu k'_\nu + k'_\mu k_\nu - k \cdot k' g_{\mu\nu}) \\ H^{\mu\nu}(p, q) &= \frac{1}{4\pi} \int d^4z e^{iq \cdot z} \langle p, s | [J_{\text{elm}}^\mu(z), J_{\text{elm}}^\nu(0)] | p, s \rangle. \end{aligned} \quad (84)$$

One now performs a Lorentz decomposition of the hadronic tensor  $H^{\mu\nu}$  and contracts it with the leptonic tensor  $L_{\mu\nu}$  (setting  $m_e = 0$ ). The differential cross section then depends on two invariant structure functions  $F_1, F_2$  (in the photon case), which are themselves functions of the scalars  $p \cdot q$ ,  $q^2$  or  $\nu$ ,  $Q^2$  or  $x, Q^2$ :

$$\frac{d^2\sigma}{dx dy} = \frac{Q^2}{y} \frac{d^2\sigma}{dx dQ^2} = \frac{4\pi\alpha^2}{xyQ^2} \left\{ \left( 1 - y - \frac{x^2 y^2 m^2}{Q^2} \right) F_2(x, Q^2) + y^2 x F_1(x, Q^2) \right\}. \quad (85)$$

Deep inelastic scattering corresponds to  $Q^2 \gg m^2$  and  $W^2 \gg m^2$ . While the cross section shows a rather complicated behaviour at low and intermediate momentum transfer, the structure functions exhibit an originally unexpected simple behaviour in the so-called Bjorken limit

$$Q^2 \gg m^2, \quad \nu \gg m \quad \text{with} \quad x = \frac{Q^2}{2m\nu} \text{ fixed}. \quad (86)$$

As shown for  $F_2$  in Fig. 15, in the Bjorken limit the structure functions seem to depend on the variable  $x$  only:

$$F_i(x, Q^2) \longrightarrow F_i(x). \quad (87)$$

This scaling behaviour suggested that the photon scatters off point-like constituents (no scale) giving rise to the quark parton model (QPM).

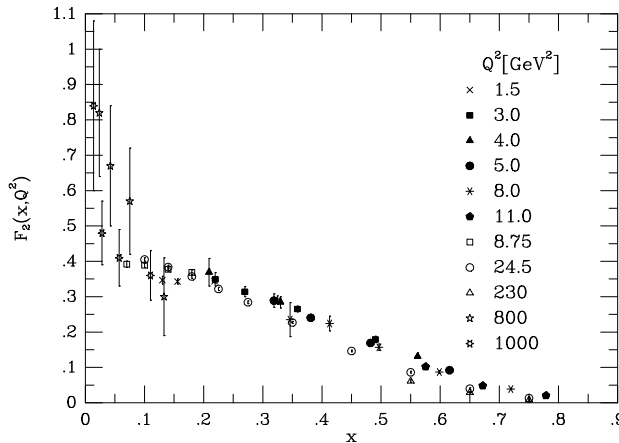


**Fig. 15:** Evidence for Bjorken scaling taken from Ref. [13].

QPM in the Breit frame

The characteristics of the QPM can best be visualized in the so-called Breit frame where the proton and the virtual photon collide head-on.



**Fig. 16:** DIS in the Breit frame.

The nucleon is pictured as a bunch of partons with negligible transverse momenta. Each parton carries a fractional momentum  $\xi p$ . Since the scattered quark is massless (compared to  $P$ ), we have

$$(q + \xi p)^2 \simeq -Q^2 + 2\xi p \cdot q = 0 \quad (88)$$

and therefore

$$\xi = x, \quad P = \frac{\sqrt{Q^2}}{2x}, \quad q + xp = (xP, -\sqrt{Q^2}/2, 0, 0). \quad (89)$$

The struck parton scatters with momentum  $q + xp$  backwards, i.e. in the direction of the virtual photon, justifying a major assumption of the QPM: the virtual photon scatters incoherently on the partons.

The fundamental process of the QPM is elastic electron-quark scattering

$$e^-(k) + q(\xi p) \rightarrow e^-(k') + q(\xi p + q). \quad (90)$$

Since there are now only two independent variables, the double differential cross section in Eq. (85) contains a  $\delta$ -function setting  $x$  equal to  $\xi$ :

$$\frac{d^2\sigma_{(q)}}{dx dy} = \frac{4\pi\alpha^2}{yQ^2} [1 + (1 - y)^2] \frac{Q_q^2}{2} \delta(x - \xi). \quad (91)$$

In the notation of Eq. (85),

$$F_{2(q)} = xQ_q^2 \delta(x - \xi) = 2xF_{1(q)}. \quad (92)$$

The incoherent sum of partonic cross sections amounts to an integral over quark distribution functions  $q(\xi), \bar{q}(\xi)$ :

$$F_2(x) = \sum_{q, \bar{q}} \int_0^1 d\xi q(\xi) x Q_q^2 \delta(x - \xi) = \sum_{q, \bar{q}} Q_q^2 x q(x), \quad (93)$$

implying the Callan-Gross relation [17]

$$F_2(x) = 2xF_1(x) \quad (94)$$

that is due to the spin-1/2 nature of quarks. The so-called longitudinal structure function  $F_L = F_2 - 2xF_1$  therefore vanishes in the QPM.

It was already known at the beginning of the seventies, before the advent of QCD, that exact scaling in the sense of the QPM was incompatible with a nontrivial QFT. QCD must therefore account for the systematic deviation from scaling that is clearly seen in the data (e.g., in Fig. 17): with increasing  $Q^2$ , the structure function  $F_2$  increases (decreases) at small (large)  $x$ .

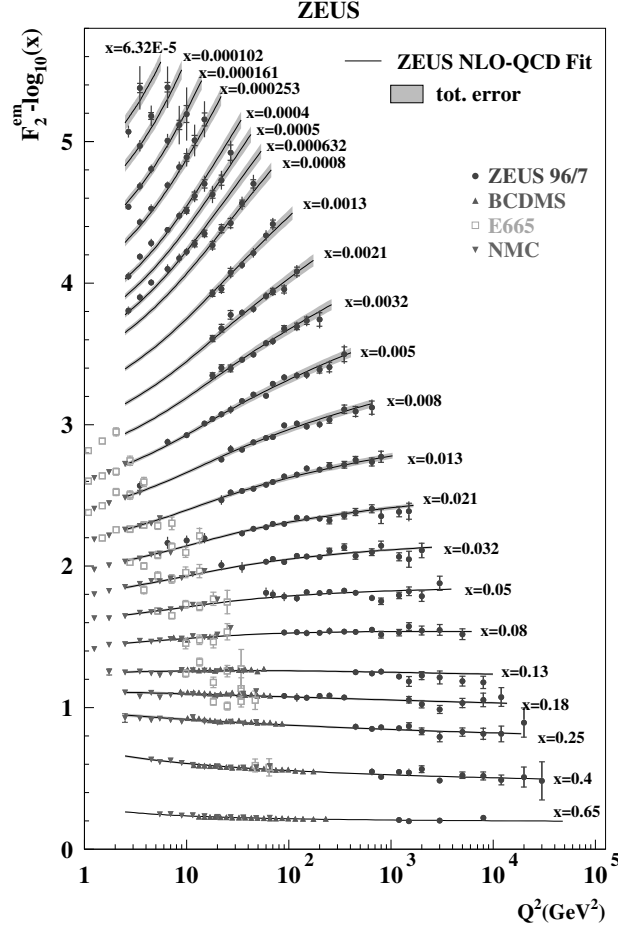


**Fig. 17:** Experimental evidence for the violation of Bjorken scaling taken from Ref. [18].

Qualitatively, scaling violation is due to the radiation of (hard) gluons generating transverse momenta for the quarks. More gluons are radiated off when  $Q^2$  increases, leading to logarithmic scaling violations in the structure functions and to scale dependent parton distribution functions (pdf)  $q_i(x, \mu^2)$ ,  $g(x, \mu^2)$  as we will now discuss in more detail.

### DIS in QCD

In QCD at leading order in  $g_s$ , the same diagrams need to be considered as the ones in Figs. 6, 7 relevant for  $e^+e^- \rightarrow \text{hadrons}$  except for crossing.

Previously, the sum of real and virtual gluon emission was infrared finite because a sum over all final state quarks and gluons was involved. In DIS the situation is different because the initial state contains a quark. Since different incoming quark momenta are in principle distinguishable, gluons collinear with the incoming quark generate in fact an infrared divergence. How to get rid of this divergence will be discussed later but for now we regulate the infrared divergence with a cutoff on the transverse quark momentum  $k_\perp^2 \geq \kappa^2$ . Adding the contribution to  $F_{2(q)}$  from real gluon emission ( $\xi = 1$  for simplicity) one finds

$$F_{2(q)}(x, Q^2) = Q_q^2 x \left[ \delta(1-x) + \frac{\alpha_s}{2\pi} \left( P_{qq}(x) \log \frac{Q^2}{\kappa^2} + C_q(x) \right) \right]. \quad (95)$$

Introduction of the cutoff  $\kappa$  has produced a logarithmic dependence on  $Q^2$ . This dependence is governed by the so-called quark-quark splitting function  $P_{qq}(x)$ . This function is universal, in contrast to the non-logarithmic coefficient function  $C_q(x)$  that is scheme dependent.

The origin of the scheme-independent  $\log Q^2$  can be understood as follows. The struck quark acquires a transverse momentum  $k_\perp$  with probability  $\alpha_s \frac{dk_\perp^2}{k_\perp^2}$ . Since  $k_\perp^2$  cannot be bigger than  $Q^2$ , integrating over all  $k_\perp$  produces the term  $\alpha_s \log Q^2 / \kappa^2$ . Virtual gluon contributions (diagrams in Fig. 7) must still be added and they are ultraviolet finite as before. Since this is a contribution from elastic scattering it must be proportional to  $\delta(1-x)$ . Altogether, the quark-quark splitting function at leading order is

$$P_{qq}(x) = \frac{4}{3} \left( \frac{1+x^2}{[1-x]_+} \right) + 2\delta(1-x). \quad (96)$$

Also the first part of  $P_{qq}(x)$  is actually a distribution. The distribution  $[F(x)]_+$  is defined in such a way that for every sufficiently regular (test) function  $f(x)$  one has

$$\int_0^1 dx f(x) [F(x)]_+ = \int_0^1 dx (f(x) - f(1)) F(x). \quad (97)$$

It is then straightforward to show that  $P_{qq}(x)$  in Eq. (96) can also be written as

$$P_{qq}(x) = \frac{4}{3} \left[ \frac{1+x^2}{(1-x)} \right]_+. \quad (98)$$

The problem remains how to interpret (or rather get rid of) the infrared cutoff  $\kappa$ . Up to now, we have only considered the quark structure function  $F_{2(q)}(x, Q^2)$ . To get  $F_2(x, Q^2)$  for the nucleon, we convolute  $F_{2(q)}(\frac{x}{\xi}, Q^2)$  with a (bare) pdf  $q_0(\xi)$ :

$$F_2(x, Q^2) = x \sum_{q, \bar{q}} Q_q^2 \left[ q_0(x) + \frac{\alpha_s}{2\pi} \int_x^1 \frac{dy}{y} q_0(y) \left\{ P_{qq}(x/y) \log \frac{Q^2}{\kappa^2} + C_q(x/y) \right\} \right]. \quad (99)$$

One now absorbs the collinear singularity  $\sim \log \kappa^2$  into  $q_0(x)$  at a factorization scale  $\mu$  to define a renormalized pdf  $q(x, \mu^2)$ :

$$q(x, \mu^2) = q_0(x) + \frac{\alpha_s}{2\pi} \int_x^1 \frac{dy}{y} q_0(y) \left\{ P_{qq}(x/y) \log \frac{\mu^2}{\kappa^2} + C'_q(x/y) \right\}. \quad (100)$$

The interpretation of  $q(x, \mu^2)$  is straightforward: the soft part  $k_\perp^2 \leq \mu^2$  is now included in the pdf. Since the scale  $\mu$  is arbitrary, the renormalized pdf is necessarily scale dependent, in complete analogy with the renormalization of ultraviolet divergences. As a small aside, we take note that the coefficient function  $C'_q$  need not be the same as  $C_q$  in Eq. (95), both being scheme dependent. The final form for the nucleon structure function  $F_2$  in the  $\overline{\text{MS}}$  scheme (except for a contribution from the gluon pdf) is then

$$\begin{aligned} F_2(x, Q^2) &= x \sum_{q, \bar{q}} Q_q^2 \int_x^1 \frac{dy}{y} q(y, \mu^2) \left[ \delta(1-x/y) + \frac{\alpha_s}{2\pi} \left\{ P_{qq}(x/y) \log \frac{Q^2}{\mu^2} + C_q^{\overline{\text{MS}}}(x/y) \right\} \right] \\ &= x \sum_{q, \bar{q}} Q_q^2 \int_x^1 \frac{dy}{y} q(y, Q^2) \left[ \delta(1-x/y) + \frac{\alpha_s}{2\pi} C_q^{\overline{\text{MS}}}(x/y) \right]. \end{aligned} \quad (101)$$

This factorization formula can be proven to all orders in  $\alpha_s$ , separating the calculable hard part from the soft part contained in the scale dependent pdfs. The pdfs  $q(x, \mu^2)$ ,  $\bar{q}(x, \mu^2)$ ,  $g(x, \mu^2)$  describe the



composition of nucleons and are, of course, not calculable in perturbation theory. They can be extracted from experimental data with the help of appropriate parametrizations (cf., e.g., Ref. [13]) but the question remains what the factorization result (101) is actually good for.

The answer is that even though the functional dependence of the pdfs cannot be calculated their scale dependence is calculable in QCD perturbation theory. The derivation of the so-called DGLAP evolution equations [19] is very similar to the derivation of the  $\beta$  function in Sec. 1.1, starting from the observation that the measurable structure function must be scale independent:

$$\mu^2 \frac{dF_2(x, Q^2)}{d\mu^2} = 0 \quad \longrightarrow \quad \mu^2 \frac{dq(x, \mu^2)}{d\mu^2} = \frac{\alpha_s(\mu)}{2\pi} \int_x^1 \frac{dy}{y} P_{qq}(x/y, \alpha_s(\mu)) q(y, \mu^2) \quad (102)$$

$$P_{qq}(x, \alpha_s(\mu)) = P_{qq}^{(0)}(x) + \frac{\alpha_s(\mu)}{2\pi} P_{qq}^{(1)}(x) + \dots \quad (103)$$

With  $P_{qq}^{(0)}(x)$  given by Eq. (98), the evolution equation at leading order takes the explicit form

$$\mu^2 \frac{dq(x, \mu^2)}{d\mu^2} = \frac{2\alpha_s(\mu)}{3\pi} \int_x^1 \frac{dz}{z} q(x/z, \mu^2) \frac{1+z^2}{1-z} - \frac{2\alpha_s(\mu)}{3\pi} q(x, \mu^2) \int_0^1 dz \frac{1+z^2}{1-z}. \quad (104)$$

Due to soft gluons, both terms on the right-hand side are divergent: the first term with positive sign is due to quarks with momentum fraction larger than  $x$  radiating off gluons whereas the second term leads to a decrease from quarks with given  $x$  that radiate gluons. The overall result is finite.

At  $O(\alpha_s)$  also the gluon pdf enters via  $\gamma^* + g \rightarrow q + \bar{q}$ . At any order, the DGLAP equations are in general  $(2N_F + 1)$ -dimensional matrix equations for  $q_i(x, \mu^2)$ ,  $\bar{q}_i(x, \mu^2)$  ( $i = 1, \dots, N_F$ ),  $g(x, \mu^2)$  with splitting functions  $P_{qq}(x)$ ,  $P_{qg}(x)$ ,  $P_{gq}(x)$  and  $P_{gg}(x)$ . The analytic calculation of these splitting functions to next-to-next-to-leading order (three loops) has just been completed [20] allowing for precise tests of scaling violations. Finally, we note that the longitudinal structure function  $F_L(x, Q^2)$  that was zero in the QPM is generated in QCD already at  $O(\alpha_s)$ .

For more applications of perturbative QCD I refer once again to the book of Ellis, Stirling and Webber [13]: jets in  $e^+e^-$  and hadroproduction, vector boson production (Drell-Yan), heavy quark production and decays, Higgs production at the LHC, ...

### 3 Heavy and light quarks

#### 3.1 Effective field theories

Unlike QED, QCD is valid down to shortest distances because of asymptotic freedom. However, at long distances where quarks and gluons are practically invisible, perturbative QCD is not applicable and a nonperturbative approach is needed. Many models can be found in the literature that are more or less inspired by QCD. Qualitative insights into the structure of the strong interactions have been found from model studies but quantitative predictions require methods that can be related directly to QCD. There are essentially only two approaches that satisfy this criterion.

- ✦ Lattice QCD has already scored impressive results and may in the long run be the most predictive method. At present, the range of applicability is still limited.
- ✦ Effective field theories (EFTs) are the quantum field theoretical formulation of the “quantum ladder”: the relevant degrees of freedom depend on the typical energy of the problem. EFTs become practical tools for phenomenology when the characteristic energy scales are well separated.

Let a given step of the quantum ladder be characterized by an energy scale  $\Lambda$ . The region  $E > \Lambda$  is the short-distance region where the fundamental theory is applicable. At long distances ( $E < \Lambda$ ), on the

other hand, an effective QFT can and sometimes must be used. By definition, the notions “fundamental” and “effective” only make sense for a given energy scale  $\Lambda$ . As we probe deeper into the physics at short distances, today’s fundamental theory will become an effective description of an even more fundamental underlying theory.

To understand the different effective field theories that are being used in particle physics, it is useful to classify them as to the structure of the transition between the fundamental and the effective level.

- Complete decoupling

The heavy degrees of freedom (heavy with respect to  $\Lambda$ ) are integrated out, i.e., they disappear from the spectrum of states that can be produced with energies  $< \Lambda$ . Correspondingly, the effective Lagrangian contains only light fields (once again, light stands for masses  $< \Lambda$ ) and may be written symbolically as

$$\mathcal{L}_{\text{eff}} = \mathcal{L}_{d \leq 4} + \sum_{d > 4} \frac{1}{\Lambda^{d-4}} \sum_{i_d} g_{i_d} O_{i_d}. \quad (105)$$

The first part  $\mathcal{L}_{d \leq 4}$  contains all the renormalizable couplings for the given set of fields. The best-known example for such a Lagrangian is the Standard Model itself. The second part of the Lagrangian (105) contains the nonrenormalizable couplings having operator dimension  $d > 4$ . The best-known example here is the Fermi theory of weak interactions with  $d = 6$  and  $\Lambda = M_W$ . For the Standard Model, on the other hand, we do not know the scale where new physics will appear. Present experimental evidence implies  $\Lambda > 100$  GeV but there are good reasons to expect new physics around  $\Lambda \sim 1$  TeV.

- Partial decoupling

In this case, heavy fields do not disappear completely in the EFT. Via so-called field redefinitions, only the high-momentum modes are integrated out. The main application of this scenario in particle physics is for heavy quark physics.

- Spontaneous symmetry breaking (SSB)

In the previous two classes, the transition from the fundamental to the effective level was smooth. Some of the fields or at least their high-energy modes just drop out and the effective description involves the remaining fields only. In the present case, the transition is more dramatic and involves a phase transition: SSB generates new degrees of freedom, the (pseudo-)Goldstone bosons associated with spontaneously broken symmetries (to be discussed in more detail in Sec. 3.4). The prefix pseudo accounts for the frequent case that the symmetry in question is not only spontaneously but also explicitly broken. Goldstone bosons in the strict sense are massless and the associated SSB relates processes with different numbers of Goldstone bosons. As a consequence, the distinction in the Lagrangian (105) between renormalizable ( $d \leq 4$ ) and nonrenormalizable ( $d > 4$ ) terms becomes meaningless. Therefore, EFTs in this category are generically nonrenormalizable. An important but maybe too simple exception is the Higgs model for electroweak SSB.

The generic EFT Lagrangian is organized in the number of derivatives of Goldstone fields and in the number of terms with explicit symmetry breaking. An important concept is universality: it turns out that EFTs describing different physical situations have very similar structure. In QCD, the symmetry in question is chiral symmetry that becomes exact in the limit of massless quarks. In the real world, SSB of chiral symmetry generates pseudo-Goldstone bosons that are identified with the pseudoscalar mesons  $\pi, K, \eta$ .

We are used to derive quantitative predictions from renormalizable QFTs in the framework of perturbation theory but how should we treat nonrenormalizable EFTs? The clue to the answer is Goldstone’s

theorem [21] that makes two crucial predictions. The first prediction is well known: SSB implies the existence of massless Goldstone bosons. The second consequence of Goldstone's theorem is not that well known but very important as well: Goldstone bosons decouple when their energies tend to zero. In other words, independently of the strength of the underlying interaction (the strong interaction in our case!), Goldstone bosons interact only weakly at low energies. This important feature allows for a systematic expansion of strong amplitudes even in the confinement regime, which is precisely the low-energy regime of QCD.

However, in contrast to the decoupling case (e.g., in heavy quark physics), the coupling constants of the low-energy EFT cannot be obtained by perturbative matching with the underlying theory of QCD. Other methods have to be used to get access to the low-energy couplings.

### 3.2 Heavy quarks

Quarks cannot be put on a balance, or more realistically, their energies and momenta cannot be measured directly. How do we then determine their masses? Two methods have been used.

- ✦ The first approach ignores confinement and calculates the pole of the quark propagator just as we determine at least in theory the mass of the electron. This looks rather artificial because the full quark propagator should have no pole because of confinement. Going ahead nevertheless, one expects those pole masses to be very much affected by nonperturbative infrared effects. In practice, this method is only used for the top quark with [14]

$$m_t = 174.3 \pm 5.1 \text{ GeV} . \quad (106)$$

- ✦ Quark masses are parameters of the QCD Lagrangian just like the strong coupling constant  $g_s$ . One therefore studies the influence of these parameters on measurable quantities and extracts specific values for the masses by comparison with experimental measurements. As for the strong coupling constant, renormalization is crucial and introduces a scale dependence also for quark masses. The scale dependence is governed by a differential equation very similar to the renormalization group equations (9) or (69) for the strong coupling:

$$\mu \frac{dm_q(\mu)}{d\mu} = -\gamma(\alpha_s(\mu))m_q(\mu) \quad (107)$$

where the anomalous dimension  $\gamma$  is nowadays known up to four-loop accuracy:

$$\gamma(\alpha_s) = \sum_{n=1}^4 \gamma_n \left( \frac{\alpha_s}{\pi} \right)^n . \quad (108)$$

The solution of this renormalization group equation for  $m_q(\mu)$  is flavour independent (in the  $\overline{\text{MS}}$  scheme):

$$m_q(\mu_2) = m_q(\mu_1) \exp \left\{ - \int_{\alpha_s(\mu_1)}^{\alpha_s(\mu_2)} dx \frac{\gamma(x)}{2\beta(x)} \right\} . \quad (109)$$

Since  $\gamma(\alpha_s)$  is positive, quark masses decrease with increasing scale  $\mu$ , e.g.,

$$\frac{m_q(1 \text{ GeV})}{m_q(M_Z)} = 2.30 \pm 0.05 . \quad (110)$$

Different methods have been used to determine the quark masses: H(eavy) Q(uark) E(ffective) T(theory) (see below), QCD sum rules (section 3.3), lattice QCD, ... The current state is summarized in Fig. 18 taken from Ref. [22]. All values correspond to the  $\overline{\text{MS}}$  scheme: light quarks are given at the scale 2 GeV whereas the heavy quarks  $m_c, m_b$  are listed as  $m_q(m_q)$ .

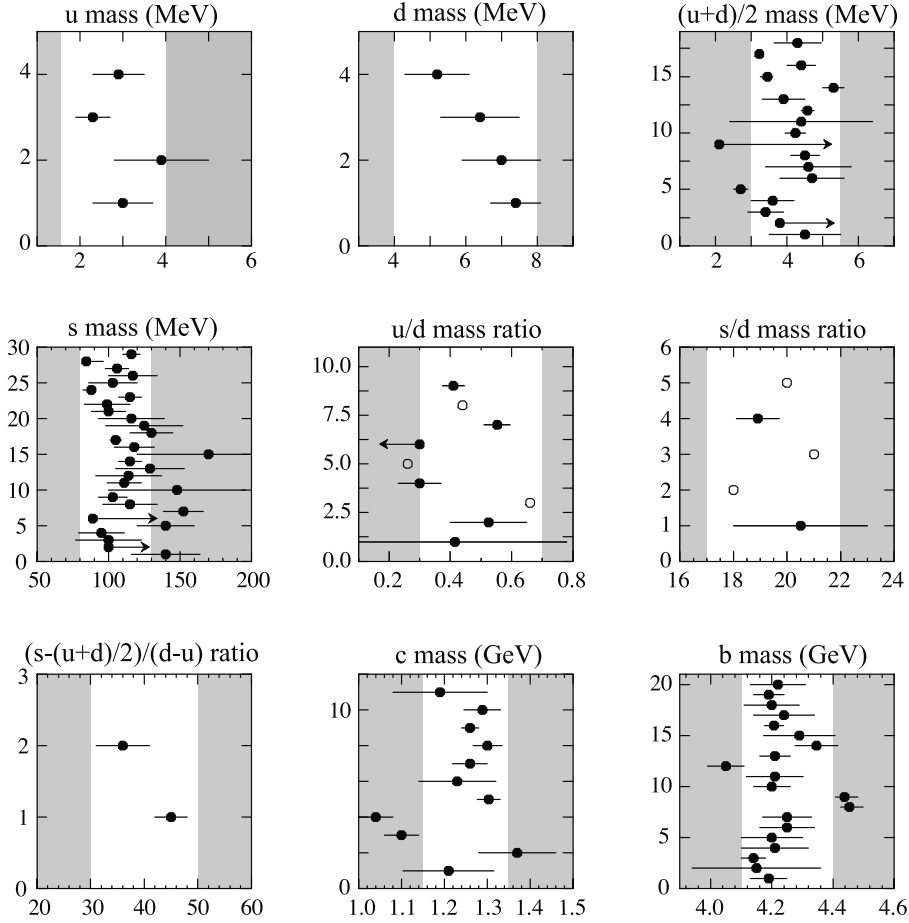


**Fig. 18:** The values of quark masses taken from the 2004 Review of Particle Properties [22]. The most recent data points are at the top of each plot.

### Heavy quark effective theory (HQET)

Why should one use an EFT for  $b$ -quark physics? After all, QCD is still accessible in perturbation theory for  $\mu = m_b$ . The main arguments in favour of HQET are the following.

- ✦ Although the hard effects are calculable in QCD perturbation theory, there are inevitably incalculable soft effects because hadrons rather than quarks and gluons appear in the final states of  $B$  decays. The necessary separation between perturbative and nonperturbative contributions is much easier to achieve in an EFT description. The keyword is the same as in deep inelastic scattering: factorization.
- ✦ Approximate symmetries that are hidden in full QCD become manifest in an expansion in  $1/m_Q$ .
- ✦ Explicit calculations simplify in general, in particular the resummation of large logs via renormalization group equations.

The physics behind HQET can be understood by an analogy with atomic physics. The spectrum of the hydrogen atom is to a good approximation insensitive to the proton mass. In fact, the atomic spectra of

hydrogen and deuterium are practically identical. The implementation of this analogy is most straightforward for hadrons with a single heavy quark ( $b$  or  $c$ ). In the hadron rest frame the heavy quark “just sits there” acting as a colour source just as the proton acts as a Coulomb source in the hydrogen atom.

We decompose the momentum of the heavy quark as

$$p^\mu = m_Q v^\mu + k^\mu, \quad (111)$$

where  $v$  is the hadron velocity normalized to  $v^2 = 1$  ( $v = (1, 0, 0, 0)$  in the hadron rest frame). The residual quark momentum  $k$  is then expected to be of  $O(\Lambda_{\text{QCD}})$  only. Starting from the QCD Lagrangian for a heavy quark  $Q$ ,

$$\mathcal{L}_Q = \bar{Q}(i\not{D} - m_Q)Q, \quad (112)$$

we decompose the quark field  $Q(x)$  into two fields  $h_v(x)$  and  $H_v(x)$  by using energy projectors  $P_v^\pm = (1 \pm \not{v})/2$  and applying (shift) factors  $e^{im_Q v \cdot x}$ :

$$\begin{aligned} Q(x) &= e^{-im_Q v \cdot x} (h_v(x) + H_v(x)) \\ h_v(x) &= e^{im_Q v \cdot x} P_v^+ Q(x), \quad H_v(x) = e^{im_Q v \cdot x} P_v^- Q(x). \end{aligned} \quad (113)$$

It is easy to check that in the hadron rest frame the fields  $h_v$  and  $H_v$  are just the upper (big) and lower (small) components of the spinor field  $Q$ , respectively. Expressing  $\mathcal{L}_Q$  in terms of  $h_v$  and  $H_v$ , one finds

$$\begin{aligned} \mathcal{L}_Q &= \bar{Q}(i\not{D} - m_Q)Q \\ &= \bar{h}_v i v \cdot D h_v - \bar{H}_v (i v \cdot D + 2m_Q) H_v + \text{mixed terms}. \end{aligned} \quad (114)$$

For the purpose of illustration, we use the field equation  $(i\not{D} - m_Q)Q = 0$  to eliminate  $H_v$  in this Lagrangian:

$$\mathcal{L}_Q = \bar{h}_v i v \cdot D h_v + \bar{h}_v i\not{D}_\perp \frac{1}{i v \cdot D + 2m_Q - i\epsilon} i\not{D}_\perp h_v \quad \text{with} \quad D_\perp^\mu = (g^{\mu\nu} - v^\mu v^\nu) D_\nu. \quad (115)$$

The heavy quark mass  $m_Q$  has disappeared from the kinetic term of the shifted field  $h_v$  and has moved to the denominator of a nonlocal Lagrangian that is in fact the starting point for a systematic expansion in  $1/m_Q$ .

The Lagrangian for  $b$  and  $c$  quarks to leading-order in  $1/m_Q$  is therefore

$$\mathcal{L}_{b,c} = \bar{b}_v i v \cdot D b_v + \bar{c}_v i v \cdot D c_v. \quad (116)$$

This Lagrangian exhibits two important symmetries. The symmetries are only approximate because the Lagrangian (116) is not full QCD but the first approximation in an expansion in  $1/m_Q$ . The symmetries are manifest in (116) but they are hidden in full QCD.

- ✦ A heavy-flavour symmetry  $SU(2)$  relates  $b$  and  $c$  quarks moving with the same velocity.
- ✦ Because there is no Dirac matrix in the Lagrangian (116), both spin degrees of freedom couple to gluons in the same way. Together with the flavour symmetry, this leads to an overall spin-flavour symmetry  $SU(4)$ .

The simplest spin-symmetry multiplet  $\mathcal{M}$  consists of a pseudoscalar  $M$  and a vector meson  $M^*$ . One of the first important applications of spin-flavour symmetry was for the semileptonic decays  $B \rightarrow D^{(*)} l \nu_l$ . In general, there are several form factors governing the two matrix elements (for  $D$  and  $D^*$ ). To leading order in  $1/m_Q$ , all those form factors are given up to Clebsch-Gordan coefficients by a single function  $\xi(v \cdot v')$  called Isgur-Wise function:

$$\langle \mathcal{M}(v') | \bar{h}_{v'} \Gamma h_v | \mathcal{M}(v) \rangle \sim \xi(v \cdot v'). \quad (117)$$

Moreover,  $\bar{h}_v \gamma^\mu h_v$  is the conserved current of heavy-flavour symmetry. Similar to electromagnetic form factors that are normalized at  $q^2 = 0$  due to charge conservation, the Isgur-Wise function is fixed in the no-recoil limit  $v = v'$  to be

$$\xi(v \cdot v' = 1) = 1. \quad (118)$$

Of course, there are corrections to this result valid only in the symmetry limit, both of  $O(\alpha_s)$  and in general of  $O(1/m_Q)$ . For the decay  $B \rightarrow D^* l \nu_l$ , the leading mass corrections turn out to be of  $O(1/m_Q^2)$  only. HQET provides the standard method for the determination of the CKM matrix element  $V_{cb}$  (see Ref. [23] for reviews).

HQET has been extended in several directions.

- Soft collinear effective theory (SCET)

HQET cannot be applied to decays like  $B \rightarrow X_s \gamma$  or  $B \rightarrow \pi \pi$  where the light particles in the final state can have momenta of  $O(m_Q)$ . SCET accounts for those energetic light states but it is more complicated than HQET. Because of the presence of several scales, several effective fields must be introduced by successive field transformations. A major achievement is again the proof of factorization that is for instance crucial for a reliable extraction of the CKM matrix element  $V_{ub}$  from experiment.

- Nonrelativistic QCD (NRQCD)

This extension of HQET includes quartic interactions to treat heavy quarkonia  $\bar{b}b$  and  $\bar{c}c$ . In this case, three widely separate scales are involved: the heavy mass  $m_Q$ , the bound-state momentum  $p \sim m_Q v$  ( $v \ll 1$ ) and the kinetic energy  $E \sim m_Q v^2$ . Applications include the analysis of the  $q\bar{q}$  potential and the production and decay of quarkonia [24].

### 3.3 QCD sum rules

The general idea of QCD sum rules is to use the analyticity properties of current correlation functions to relate low-energy hadronic quantities to calculable QCD contributions at high energies. We recall the example of the two-point functions  $\Pi_L^{(0,1)}(q^2)$  in hadronic  $\tau$  decays discussed in Sec. 2.4.

In general, the QCD contribution consists itself of two different parts,

- a purely perturbative part and
- a partly nonperturbative part that is important at intermediate energies and makes use of the operator product expansion (OPE, another case of factorization).

Altogether, a typical two-point function (QCD sum rules are not restricted only to two-point functions, however) has the form

$$\Pi(q^2) = \Pi_{\text{pert}}(q^2) + \sum_d C_d(q^2) \langle 0 | O_d | 0 \rangle. \quad (119)$$

The so-called Wilson coefficients  $C_d(q^2)$  are calculable perturbatively and they depend on the two-point function under consideration. Up to logs, they decrease for large  $|q^2|$  as  $(q^2)^{-n(d)}$  with some positive integer  $n(d)$ . The vacuum condensates  $\langle 0 | O_d | 0 \rangle$ , on the other hand, are universal and they absorb long-distance contributions with characteristic momenta  $< \sqrt{|q^2|}$ .

Three main types of applications of QCD sum rules can be distinguished.

- Using experimental data as input for the low-energy hadronic part, one can extract universal QCD parameters:  $\alpha_s$ , quark masses, condensates, ...

- With QCD parameters known, one can predict hadronic quantities: hadron masses, decay constants, amplitudes, ...
- The compatibility of low-energy data with QCD can be checked. I will discuss a recent example of topical interest, the spectral data relevant for the leading hadronic contribution to the anomalous magnetic moment of the muon.

$$(g - 2)_\mu$$

The biggest source of uncertainty in the calculation of the anomalous magnetic moment of the muon  $a_\mu = (g_\mu - 2)/2$  in the Standard Model is at present the lowest-order hadronic vacuum polarization

$$a_\mu^{\text{had,LO}} = a_\mu^{\text{vac.pol.}} = \int_{4M_\pi^2}^{\infty} dt K(t) \sigma_0(e^+e^- \rightarrow \text{hadrons})(t) \quad (120)$$

depicted in Fig. 19.

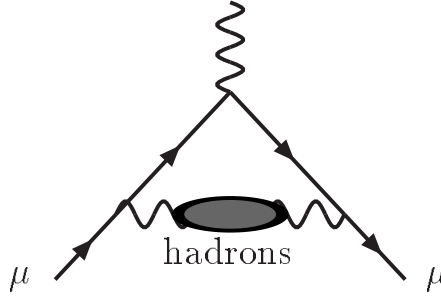


**Fig. 19:** Lowest-order hadronic vacuum polarization contribution to the anomalous magnetic moment of the muon.

The kernel  $K(t)$  is a known function [25]. Although the integral extends from threshold to infinity, about 73 % of  $a_\mu^{\text{had,LO}}$  are due to the  $\pi\pi$  intermediate state in Fig. 19, governed by the pion form factor. Moreover, 70 % of  $a_\mu^{\text{had,LO}}$  come from the region  $t \leq 0.8 \text{ GeV}^2$ . Therefore, by far the most important part is not calculable in QCD perturbation theory.

A few years ago, Alemany, Davier and Höcker [26] suggested to use not only data from  $e^+e^- \rightarrow \pi^+\pi^-$  to extract the pion form factor but also from the decay  $\tau^- \rightarrow \pi^0\pi^-\nu_\tau$ . In the isospin limit, it is straightforward to derive the relation

$$\sigma_0(e^+e^- \rightarrow \pi^+\pi^-)(t) = h(t) \frac{d\Gamma(\tau^- \rightarrow \pi^0\pi^-\nu_\tau)}{dt} \quad (121)$$

with a known function  $h(t)$  where  $t$  is the two-pion invariant mass squared.

At the level of precision required for comparison with experiment (better than 1 % for  $a_\mu^{\text{had,LO}}$ ), isospin violating and electromagnetic corrections are mandatory [27, 28]. The status until recently was summarized by Höcker at the High Energy Conference in Beijing [29].

- ☛ There was a significant discrepancy between the  $\tau$  and  $e^+e^-$  data, mainly above the  $\rho$  resonance region, as shown in Fig. 20.

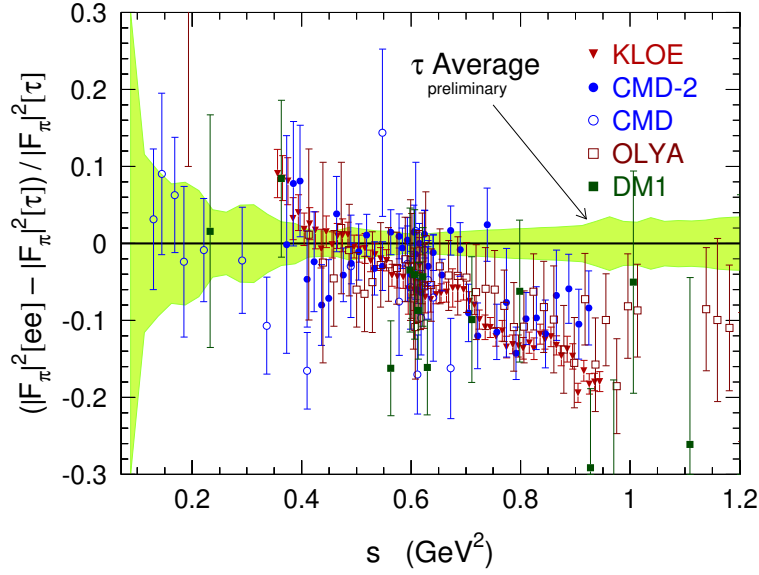


**Fig. 20:** Comparison between  $e^+e^-$  and  $\tau$  data for the pion form factor from Ref. [29]; plotted is the difference of the form factors squared normalized to the  $\tau$  data.

- ✦ Isospin violation cannot explain the difference.
- ✦ The  $e^+e^-$  data from the KLOE experiment confirm the previous trend of the CMD-2 data although the agreement among the  $e^+e^-$  data is not impressive.

The widely accepted recommendation at the Beijing Conference was to ignore the  $\tau$  data until the origin of the discrepancy is understood [29].

The situation has changed both on the theoretical and on the experimental side. The theoretical clarification is due to Maltman [30] who checked the consistency of experimental data with QCD by investigating sum rule constraints for the two spectral functions relevant for the  $e^+e^-$  and the  $\tau$  case, respectively:

$$\rho_{\text{em}}(s) = \text{Im } \Pi_{\text{elm}}(s) \quad \text{and} \quad \rho_V^{I=1}(s) = \text{Im } \Pi_{L,ud}(s) .$$

By using a contour integral in the complex  $s$ -plane as in Fig. 13, with  $m_\tau^2$  replaced by an a priori arbitrary  $s_0$ , one derives a so-called F(inite)E(nergy)S(um)R(ule)

$$\int_0^{s_0} w(s) \rho(s) ds = -\frac{1}{2\pi} \oint_{|s|=s_0} w(s) \Pi(s) ds . \quad (122)$$

$\Pi(s)$ ,  $\rho(s)$  refer to the two cases considered (electromagnetic currents in the  $e^+e^-$  case, charged currents for  $\tau$ ) and  $w(s)$  is an analytic function (actually a polynomial) that will be chosen conveniently.

The right-hand side of the FESR can be estimated in QCD as exemplified by Eq. (119). The purely perturbative part is known up to  $\alpha_s^3$ , with estimates of the  $O(\alpha_s^4)$  contribution available. For not too small  $s_0$  the purely perturbative part dominates the right-hand side depending only on  $\alpha_s(M_Z)$ . The  $d = 2$  part is completely negligible in the  $\tau$  case and it depends only on the mass of the strange quark in the electromagnetic case. The  $d = 4$  contributions involve the quark condensates  $\langle 0 | m_q \bar{q} q | 0 \rangle$  ( $q = u, d, s$ ) (very well known from chiral perturbation theory, cf. Sec. 3.5) and the gluon condensate  $\langle 0 | \alpha_s G_{\mu\nu}^a G_a^{\mu\nu} | 0 \rangle$  (less well but sufficiently known from charmonium sum rules). For  $d \geq 6$ , the relevant condensates are practically unknown. However, by using the pinching trick ( $w(s_0) = 0$ ) appropriately, Maltman eliminates the  $d = 6$  OPE contributions to  $\Pi(s)$  altogether. The negligible effect of  $d \geq 8$  contributions can be checked by varying  $s_0$ .



Turning now to the left-hand side of the FESR (122), Maltman uses the most precise experimental data for the spectral functions: ALEPH (compatible with CLEO and OPAL) for  $\rho_V^{I=1}(s)$ , CMD-2 for  $\rho_{\text{em}}(s)$ . As a first test, he fits  $\alpha_s(M_Z)$  (keeping the remaining OPE input fixed) from the experimentally determined left-hand side of the FESR. The outcome is, quite independently of the weight function  $w(s)$  that is always chosen positive and monotonically increasing for  $0 \leq s \leq s_0$ , that the fitted value of  $\alpha_s(M_Z)$  is systematically lower than the high-energy determination dominated by LEP in the electromagnetic case while there is perfect agreement in the  $\tau$  case. This is a first indication that the electromagnetic spectral density is too low.

A second test, largely independent of the value of  $\alpha_s(M_Z)$ , compares the slopes of the OPE parts and spectral integrals with respect to  $s_0$ . The results are shown in Figs. 21, 22.

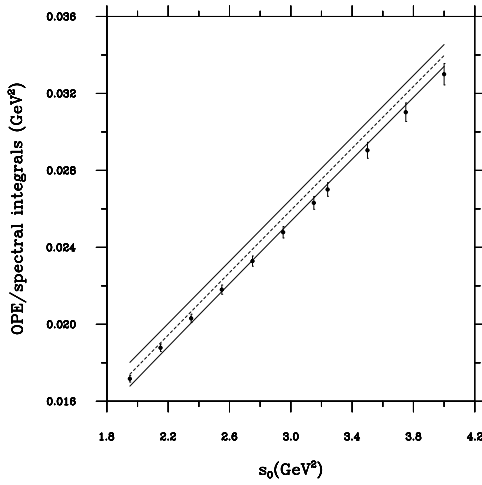


**Fig. 21:** Slopes with respect to  $s_0$  in the  $e^+e^-$  case for a specific weight function  $w_6(s)$ . The dashed lines denote the central values for the OPE input and the solid lines indicate the error bands. The spectral integrals are shown for several points, error bars included.

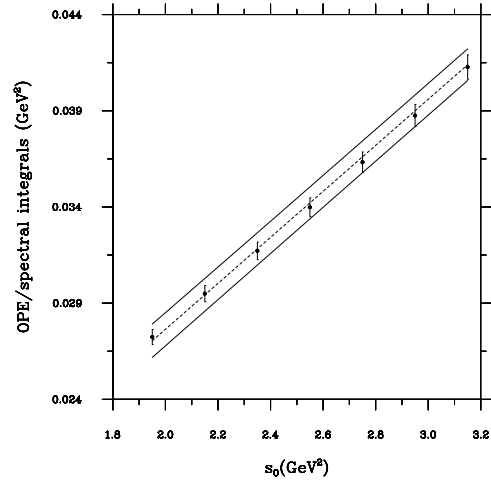


**Fig. 22:** Same as in the previous figure for the  $\tau$  data. Both figures are taken from Ref. [30].

The situation is similar as before. While the slopes differ between data and QCD by  $\gtrsim 2.5\sigma$  in the electromagnetic case there is perfect agreement in the  $\tau$  case. The previous conclusion is reinforced: the  $e^+e^-$  spectral data are systematically too low whereas the  $\tau$  data are completely consistent with QCD, both in normalization and in the slopes. The QCD sum rule tests clearly favour the  $\tau$  over the  $e^+e^-$  data for the pion form factor.

The most recent development is again an experimental one. Only two months before the School new data on  $e^+e^- \rightarrow \pi^+\pi^-$  were released by the SND Collaboration from Novosibirsk. Their results disagree with both CMD-2 and KLOE and they go in the right direction towards reconciling the  $e^+e^-$  with the  $\tau$  data. The discrepancies between the three data sets in  $e^+e^-$  annihilation remain to be understood. Based on  $\tau$  data for the  $2\pi$  and  $4\pi$  channels in the hadronic vacuum polarization, the calculation of the anomalous magnetic moment of the muon in the Standard Model [31] compares well with the measured value [32]:

$$a_\mu^{\text{exp}} - a_\mu^{\text{SM}} = (7.6 \pm 8.9) \cdot 10^{-10}. \quad (123)$$

There is at present no evidence for a discrepancy between the Standard Model and experiment.

### 3.4 Chiral symmetry

By construction, QCD is a gauge theory with gauge group  $SU(3)_c$ . However, the QCD Lagrangian

$$\mathcal{L}_{\text{QCD}} = -\frac{1}{2}\text{tr}(G_{\mu\nu}G^{\mu\nu}) + \sum_{f=1}^{N_F} \bar{q}_f (i\not{D} - m_f \mathbb{1}_c) q_f \quad (124)$$

possesses additional symmetries. As in QED, the theory is parity invariant because of the absence of  $\gamma_5$  (vector couplings only). Moreover, the coupling constant  $g_s$  and the quark masses  $m_f$  are real so that QCD conserves also CP, ignoring the so-called strong CP problem here.

Are there still additional symmetries in the QCD Lagrangian (124)? To answer this question, we first have a look at the quark kinetic term only (with  $N_F = 6$  flavours):

$$\mathcal{L}_{\text{kin}} = i \sum_{f=1}^6 \bar{q}_f \not{D} q_f = i \sum_{f=1}^6 \{ \bar{q}_{fL} \not{D} q_{fL} + \bar{q}_{fR} \not{D} q_{fR} \} , \quad (125)$$

with chiral components

$$q_L = \frac{1}{2}(1 - \gamma_5)q, \quad q_R = \frac{1}{2}(1 + \gamma_5)q . \quad (126)$$

Since the  $q_{fL}$  and the  $q_{fR}$  do not talk to each other in (125), they can be rotated separately implying the maximal global flavour symmetry  $U(6) \times U(6)$ . However, this is a symmetry of the kinetic term only. In the full quark Lagrangian (colour indices will be suppressed from now on)

$$\mathcal{L}_q = \sum_{f=1}^6 \{ \bar{q}_{fL} i\not{D} q_{fL} + \bar{q}_{fR} i\not{D} q_{fR} - m_f (\bar{q}_{fR} q_{fL} + \bar{q}_{fL} q_{fR}) \} \quad (127)$$

$q_{fL}$  and  $q_{fR}$  can in general not be rotated separately any longer because of the quark masses. The actual flavour symmetry therefore depends on the quark mass matrix

$$\mathcal{M}_q = \text{diag} (m_u, m_d, m_s, m_c, m_b, m_t) . \quad (128)$$

In order to find all even only approximate symmetries of QCD, we distinguish several cases depending on the specific values of the quark masses.

- i. In the real world, all quark masses are non-zero and they are all different from each other. In this case, the remaining flavour symmetry amounts to the phase transformations  $q_{fL,R} \rightarrow e^{-i\varepsilon_f} q_{fL,R}$  ( $f = 1, \dots, 6$ ) where the phase  $\varepsilon_f$  for a given flavour must be the same for  $q_{fL}$  and  $q_{fR}$ . The symmetry group reduces to the product  $U(1) \times U(1) \times \dots \times U(1) = U(1)^6$  leading to the well-known conserved flavour quantum numbers  $N_u, N_d, N_s, N_c, N_b$  and  $N_t$ . All these symmetries are broken by the weak interactions, except their sum (baryon number)

$$B = (N_u + N_d + N_s + N_c + N_b + N_t) / 3 . \quad (129)$$

- ii. In some approximation, the quark masses are still non-zero but  $n_F$  of them are equal ( $n_F < N_F = 6$ ). In this case, the maximal symmetry group  $U(6) \times U(6)$  reduces to

$$U(n_F) \times U(1)^{6-n_F} \simeq SU(n_F) \times U(1) \times U(1)^{6-n_F} . \quad (130)$$

The only realistic cases are  $n_F = 2$  or  $3$  and they lead to well-known approximate symmetries:

$$\begin{array}{lll} n_F = 2: & m_u = m_d & \longrightarrow \text{isospin } SU(2) \\ n_F = 3: & m_u = m_d = m_s & \longrightarrow \text{flavour } SU(3) \end{array}$$

- iii. A much more radical approximation consists in setting some of the quark masses to zero:  $m_f = 0$  ( $f = 1, \dots, n_F$ ). In this case,  $n_F$  of the  $q_{fL}$  and  $q_{fR}$  can again be rotated separately implying the chiral symmetry

$$SU(n_F)_L \times SU(n_F)_R \times U(1)_V \times U(1)_A [\times U(1)^{6-n_F}] . \quad (131)$$

To set  $n_F = 2$  of the quark masses to zero is a reasonable approximation in view of  $m_{u,d} \ll \Lambda_{\text{QCD}}$ , whereas  $n_F = 3$  (setting also  $m_s = 0$ ) is certainly more daring.  $U(1)_V$  is again responsible for baryon number conservation. The factor  $U(1)_A$  is actually not a symmetry of full QCD at the quantum level (abelian anomaly).

We are familiar with isospin and flavour  $SU(3)$  that we see at least approximately realized in the hadron spectrum. But what are the consequences of the approximate chiral symmetry of QCD? If chiral symmetry would manifest itself in the hadron spectrum, each hadron would have to have a partner of opposite parity of approximately the same mass. That is obviously not the case: chiral symmetry appears to be more hidden than isospin, for example. In order to understand the manifestations of chiral symmetry, we have to recall the main features of

Spontaneous symmetry breaking

There are many examples of SSB in physics and the best-known example in particle physics is the spontaneously broken electroweak symmetry (see the Lectures of W. Buchmüller at this School).

The mechanism was first realized in condensed matter physics and a good example for our purpose is the ferromagnet. The underlying theory of the ferromagnet (eventually QED) is certainly rotationally invariant. The Hamiltonian (e.g., of the Heisenberg model) does not single out any direction in space. Nevertheless, in the ground state of the ferromagnet the spins align in a certain direction. The direction is arbitrary and there is no trace of it in the Hamiltonian. In this sense rotational symmetry is “spontaneously” broken. It is certainly not manifest in the ground state but it has other important consequences such as the existence of excitations (called magnons or spin waves in this case) with a very special dispersion law. The dispersion law is the dependence of the frequency  $\omega$  on the wave length  $\lambda$  or on the wave number  $k = 2\pi/\lambda$ . SSB in condensed matter physics implies that for some excitations the frequency tends to zero for infinite wave length:

$$\lim_{k \rightarrow 0} \omega(k) = \lim_{\lambda \rightarrow \infty} \omega(k) = 0 . \quad (132)$$

This property of magnons in particular is easy to visualize as shown in Fig. 23. In the ground state of the ferromagnet spins are aligned. A typical spin wave is displayed in the second line: the wave length is the distance between spins pointing in the same direction. In the limit  $\lambda \rightarrow \infty$ , the spins become again aligned, albeit in a different direction in general. Since by the assumed rotational symmetry of the theory each direction is as good as any other, the configurations in the first and in the last line must have the same energy as expressed by Eq. (132). Put in another way, magnons do not have an energy gap in their spectrum.

What is the analogy in a relativistic QFT like QCD? The frequency is replaced by the energy of the particle, with the three-momentum instead of the wave number. The dispersion law is just the relativistic energy-momentum relation  $E = \sqrt{p^2 + m^2}$ . The energy tends to zero for  $p \rightarrow 0$  if and only if the particle is massless:

$$\lim_{p \rightarrow 0} E = \lim_{p \rightarrow 0} \sqrt{p^2 + m^2} = 0 \quad \Longleftrightarrow \quad m = 0 . \quad (133)$$

How can we distinguish if a symmetry is realized in the usual way (like isospin) or if it is spontaneously broken? The crucial question is what the conserved charge  $Q = \int d^3x J^0(x)$  associated with a symmetry current  $J^\mu(x)$  ( $\partial_\mu J^\mu = 0$ ) does when applied to the ground state (vacuum). In a relativistic quantum field theory, there are only two options:

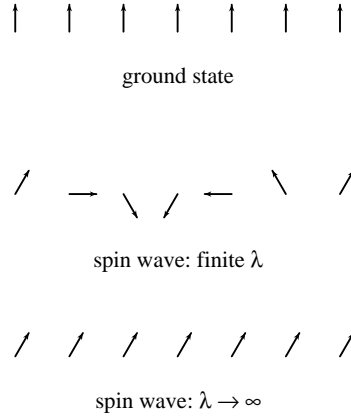


**Fig. 23:** Spin directions in the (one-dimensional) ferromagnet: ground state, spin wave with finite wave length and a spin wave with infinite wave length.

### Goldstone alternative

$Q 0\rangle = 0$	$  Q 0\rangle   = \infty$
Wigner–Weyl	Nambu–Goldstone
linear representation	nonlinear realization
degenerate multiplets	massless Goldstone bosons
exact symmetry	spontaneously broken symmetry

The left column describes the more familiar case (Wigner–Weyl) where states are grouped in multiplets (irreducible representations of the symmetry group). The vacuum is annihilated by the charge and the states in a given multiplet all have the same mass (degeneracy). In the other possible realization (Nambu–Goldstone), applying the charge to the vacuum is, strictly speaking, not defined. There are no degenerate multiplets (therefore we don’t see the symmetry in the spectrum) but there must be massless particles in the theory (Goldstone bosons). Although the charge cannot be applied to the vacuum directly, the following matrix element called an order parameter of SSB may be well defined:

$$\langle 0|[Q, A]|0\rangle \quad (134)$$

where  $A$  is some operator. If we can find an order parameter that is different from zero, the symmetry associated with the charge  $Q$  is necessarily spontaneously broken. This is easy to understand: because of the commutator in (134) the order parameter vanishes if  $Q$  annihilates the vacuum. In the familiar example of electroweak symmetry breaking, scalar field operators  $\varphi_i$  take the place of  $A$  with  $[Q, \varphi_i] = c_{ij}\varphi_j$ . If  $c_{ij}\langle 0|\varphi_j|0\rangle \neq 0$  (Higgs vacuum expectation value), the electroweak symmetry is spontaneously broken. This is also a good example that the argument goes in one direction only. Even if all scalars have zero vacuum expectation values or if there aren’t any scalar fields at all the symmetry may still be spontaneously broken. The mechanism could involve some other operator  $A$  in the order parameter (134).

For each spontaneously broken symmetry Goldstone’s theorem implies the existence of a massless state  $|G\rangle$  with

$$\langle 0|J^0(0)|G\rangle\langle G|A|0\rangle \neq 0. \quad (135)$$

A necessary and sufficient condition for SSB is that the

Goldstone matrix element  $\langle 0|J^0(0)|G\rangle \neq 0$

implying also that the Goldstone state  $|G\rangle$  has the same quantum numbers as  $J^0(0)|0\rangle$ . The following remarks are useful:

- The state  $|G\rangle$  need not correspond to a physical particle. This can only happen in the case of a spontaneously broken gauge symmetry as in electroweak theory.
- $J^0(0)$  is usually a rotationally invariant bosonic operator and thus  $|G\rangle$  carries spin 0.
- Spontaneous breaking of discrete symmetries does not give rise to Goldstone bosons.

The main features of SSB can be discussed in the original Goldstone model. It has a single complex scalar field  $\phi(x)$  with the Lagrangian

$$\mathcal{L}_{\text{Goldstone}} = \partial_\mu \phi \partial^\mu \phi^\dagger - \lambda \left( \phi \phi^\dagger - \frac{v^2}{2} \right)^2 \quad (\lambda, v \text{ real and positive}), \quad (136)$$

symmetric with respect to global  $U(1)$  transformations  $\phi(x) \rightarrow e^{i\alpha} \phi(x)$ . The minimum of the Mexican hat potential occurs at  $\phi \phi^\dagger = \frac{v^2}{2}$ . Decomposing the complex field  $\phi(x)$  into two hermitian fields  $R(x), G(x)$  with

$$\begin{aligned} \phi(x) &= (R(x) + iG(x))/\sqrt{2} \\ \langle 0|R(x)|0\rangle &= v, \quad \langle 0|G(x)|0\rangle = 0, \end{aligned} \quad (137)$$

the Lagrangian expressed in terms of the fields  $R(x), G(x)$  displays the following spectrum at tree level:

Goldstone boson field $G(x)$	$M_G = 0$
massive field $H(x) = R(x) - v$	$M_H = \sqrt{2\lambda} v$

Denoting the four-momenta of Goldstone particles generically as  $p_G$ , one finds an unexpected behaviour for scattering amplitudes: they vanish for  $p_G \rightarrow 0$ , e.g.,

$$A(GG \rightarrow GG) = O(p_G^4), \quad A(GH \rightarrow GH) = O(p_G^2) \quad (138)$$

for arbitrary values of non-Goldstone momenta  $p_H$ . More generally, Goldstone bosons decouple when their energies tend to zero.

This behaviour looks mysterious at first, but it can be understood by choosing a different set of fields. Instead of the fields  $G(x)$  and  $H(x)$ , we choose another representation (polar decomposition) that may be familiar from electroweak theory:

$$\phi(x) = \frac{1}{\sqrt{2}} [h(x) + v] e^{ig(x)/v}. \quad (139)$$

In terms of the hermitian fields  $g(x), h(x)$  the Goldstone Lagrangian takes the form

$$\begin{aligned} \mathcal{L}_{\text{Goldstone}} &= \frac{1}{2} (\partial_\mu g)^2 + \frac{1}{2v^2} (h^2 + 2vh) (\partial_\mu g)^2 \\ &+ \frac{1}{2} (\partial_\mu h)^2 - \lambda v^2 h^2 - \frac{\lambda}{4} (h^4 + 4vh^3). \end{aligned} \quad (140)$$

A general theorem of QFT ensures that the fields  $G, H$  on one side and  $g, h$  on the other side produce the same  $S$ -matrix elements although the Green functions are in general different.

The main consequences are the following.

- The particle spectrum is unchanged:

Goldstone field $g(x)$	$M_g = 0$
massive field $h(x)$	$M_h = \sqrt{2\lambda} v$

- The Goldstone field  $g$  has only derivative couplings implying for the scattering amplitudes considered previously:

$$\lim_{p_G \rightarrow 0} A(p_G) = 0 . \quad (141)$$

The important lesson is very general and not restricted to the Goldstone model.  $S$ -matrix elements with only Goldstone states vanish for  $p_G \rightarrow 0$ . When other non-Goldstone particles participate in the initial and final states, the statement remains true for some matrix elements like for elastic scattering  $GH \rightarrow GH$ . In general, the interactions of Goldstone bosons among themselves and with other matter become arbitrarily weak for small momenta.

### 3.5 Chiral perturbation theory

We start from a theorist's paradise (copyright H. Leutwyler), QCD in the chiral limit where  $n_F = 2$  [or 3] quarks  $u, d$  [,  $s$ ] are massless:

$$\mathcal{L}_{\text{QCD}}^0 = \bar{q}_L i \not{D} q_L + \bar{q}_R i \not{D} q_R + \mathcal{L}_{\text{heavy quarks}} + \mathcal{L}_{\text{gauge}} \quad (142)$$

with

$$q^\top = (u \ d \ [s]) .$$

As explained in the previous section, this Lagrangian has a global symmetry

$$SU(n_F)_L \times SU(n_F)_R \times U(1)_V \times U(1)_A [\times U(1)^{6-n_F}] . \quad (143)$$

The nonabelian factor  $G = SU(n_F)_L \times SU(n_F)_R$  is called the chiral group.

Although not yet proven from QCD alone, there is strong evidence, both from phenomenology and from theory, that chiral symmetry is spontaneously broken. The spontaneous breaking does not affect all of  $G$  but, roughly speaking, half of it:  $G \longrightarrow H = SU(n_F)_V$ . The so-called vectorial subgroup  $H$  of  $G$  is nothing but isospin (for  $n_F = 2$ ) or flavour  $SU(3)$  (for  $n_F = 3$ ) and it is realized in the familiar way à la Wigner-Weyl. Some arguments in favour of this spontaneous breakdown are:

- As already emphasized before, there are no parity doublets in the hadron spectrum.
- There is no other convincing argument why the pseudoscalar mesons are the lightest hadrons. Spontaneous chiral symmetry breaking implies that they would be massless in the chiral limit (pseudo-Goldstone bosons).
- The vector and axial-vector spectral functions are very different ( $\rho$  vs.  $a_1$ ).
- The so-called anomaly matching conditions together with confinement require that  $G$  is spontaneously broken for  $n_F \geq 3$ .
- Under very reasonable assumptions,  $SU(n_F)_V$  is not spontaneously broken. It is of course explicitly broken by the differences between quark masses.

Even if it has not been possible so far to prove directly from QCD that chiral symmetry is spontaneously broken, we can ask for possible order parameters. It turns out (more details can be found in Ref. [33], for instance) that the simplest such order parameter involves the pseudoscalar operators  $A_b = \bar{q} \gamma_5 \lambda_b q$  ( $a = 1, \dots, 8$ ) giving rise to the quark condensate  $\langle 0 | \bar{q} q | 0 \rangle$ . There is evidence both from lattice QCD and from phenomenology that the quark condensate is non-zero implying spontaneous chiral

symmetry breaking. As will be discussed in Sec. 3.7, the quark condensate is in fact the dominant order parameter of spontaneous chiral symmetry breaking, in a sense to be specified later.

From Goldstone's theorem we know (still in the chiral limit) that there are  $n_F^2 - 1$  massless Goldstone bosons:

$n_F$	$n_F^2 - 1$	Goldstone bosons
2	3	$\pi$
3	8	$\pi, K, \eta$

Although the real world is not a theorist's paradise, we still expect low-energy amplitudes to be dominated by the exchange of pseudoscalar mesons, which are the lightest hadrons also in the real world. In order to calculate such amplitudes, we construct an effective field theory with only Goldstone fields. As already explained in Sec. 3.1, the Lagrangian of Goldstone fields is nonrenormalizable and it is in fact even nonpolynomial. The underlying physical reason is that we can add any number of sufficiently soft pions (still massless!) to a hadron state without appreciably changing its energy. Therefore, we have degenerate states with different numbers of particles that are related by chiral symmetry transformations. For the Lagrangian this argument implies that the symmetry transformations are nonlinear in the pion fields. Starting from a Lagrangian with fixed powers in the Goldstone fields, successive nonlinear transformations generate any number of fields in the Lagrangian. Since the Lagrangian is to be symmetric under such transformations it must necessarily be nonpolynomial.

The basic building block of chiral Lagrangians is therefore a nonpolynomial matrix function of the Goldstone fields, e.g., the exponential function (for  $n_F = 3$ )

$$U(\phi) = \exp(i\sqrt{2}\Phi/F), \quad \Phi = \begin{pmatrix} \frac{\pi^0}{\sqrt{2}} + \frac{\eta_8}{\sqrt{6}} & \pi^+ & K^+ \\ \pi^- & -\frac{\pi^0}{\sqrt{2}} + \frac{\eta_8}{\sqrt{6}} & K^0 \\ K^- & \bar{K}^0 & -\frac{2\eta_8}{\sqrt{6}} \end{pmatrix} \quad (144)$$

where  $F$  is the pion decay constant in the chiral limit characterizing the size of the Goldstone matrix element  $\langle 0|J^0(0)|G\rangle$ .

Chiral Lagrangians are organized according to the number of derivatives of the fields. The unique lowest-order Lagrangian of  $O(p^2)$  with two derivatives is the so-called nonlinear  $\sigma$  model:

$$\mathcal{L}_2^{(0)} = \frac{F^2}{4} \text{tr}_{n_F} \left( \partial_\mu U \partial^\mu U^\dagger \right) =: \frac{F^2}{4} \langle \partial_\mu U \partial^\mu U^\dagger \rangle = \partial_\mu \pi^+ \partial^\mu \pi^- + \frac{1}{2} \partial_\mu \pi^0 \partial^\mu \pi^0 + O(\pi^4), \quad (145)$$

using a bracket notation for  $n_F$ -dimensional traces.

So much for the paradise. Back to reality, we must admit that there is no chiral symmetry in nature! In the Standard Model, it is explicitly broken in two different ways.

- Chiral symmetry is explicitly broken by nonvanishing quark masses. This should be a small modification for two, a more pronounced one for three flavours:

$$\begin{array}{lll} m_u, m_d & \ll & M_\rho & n_F = 2 \\ m_s & < & M_\rho & n_F = 3 \end{array}$$

- Also the electroweak interactions break chiral symmetry. If electroweak effects are to be included, they can be taken into account perturbatively in  $\alpha, G_F$ .

The main assumption of chiral perturbation theory (CHPT) is that an expansion around the chiral limit (the theorist's paradise) makes sense. Therefore, even in the absence of electroweak interactions, chiral Lagrangians are organized in a two-fold expansion.

- i. Spontaneous chiral symmetry breaking gives rise to an expansion in derivatives of the fields leading to an expansion of amplitudes in the momenta of pseudo-Goldstone bosons.
- ii. Explicit symmetry breaking suggests an expansion also in the quark masses  $m_q$ .

The two expansions can be related via the meson masses. As will be discussed in the next subsection, the squares of the meson masses start out linear in the quark masses:

$$M_M^2 \sim m_q + O(m_q^2) . \quad (146)$$

The standard chiral counting therefore amounts to treating quark masses like the second power of momenta:

$$m_q = O(M_M^2) = O(p^2) . \quad (147)$$

The effective Lagrangian (for pseudoscalar mesons) is therefore of the form [34]

$$\begin{aligned} \mathcal{L}_{\text{eff}} &= \mathcal{L}_2 + \mathcal{L}_4 + \mathcal{L}_6 + \dots \\ \mathcal{L}_2 &= \frac{F^2}{4} \langle \partial_\mu U \partial^\mu U^\dagger + \chi U^\dagger + \chi^\dagger U \rangle \end{aligned} \quad (148)$$

where  $\chi$  represents the quark masses:  $\chi = 2B\mathcal{M}_q = 2B \text{diag}(m_u, m_d, m_s)$ . The lowest-order Lagrangian contains only two parameters  $F, B$  that are related to physical quantities as

$$F_\pi = F [1 + O(m_q)] , \quad \langle 0 | \bar{u}u | 0 \rangle = -F^2 B [1 + O(m_q)] . \quad (149)$$

The lowest-order amplitudes of CHPT are of  $O(p^2)$  and they correspond to the current algebra amplitudes of 40 years ago. The tree-level amplitudes can be read off directly from the Lagrangian (148) depending only on  $F_\pi$  and  $M_M^2$  [ $M_\pi^2 = B(m_u + m_d), \dots$ ]. For instance, the elastic  $\pi\pi$  scattering amplitude of  $O(p^2)$  is given by

$$A_2(s, t, u) = \frac{s - M_\pi^2}{F_\pi^2} . \quad (150)$$

Contrary to symmetries like isospin that relate different amplitudes, the spontaneously broken chiral symmetry makes an absolute prediction for this scattering amplitude. It was left as an exercise to the audience to explain why that is possible.

The lowest-order results we have been discussing so far were already known in the late sixties and early seventies of the last century (current algebra, phenomenological Lagrangians). After an influential paper of Weinberg [35], but especially with the work of Gasser and Leutwyler [34] the systematic treatment of QCD at low energies became a respectable theory. The first step was to construct the Lagrangian of next-to-leading order  $\mathcal{L}_4$  that contains 10 (7) additional coupling constants (usually called LECs for low-energy constants) for  $SU(3)$  ( $SU(2)$ ). With a hermitian Lagrangian tree amplitudes are necessarily real but we know that unitarity and analyticity require complex amplitudes. It is not difficult to convince oneself that imaginary parts occur first at  $O(p^4)$ . The consequence is that a systematic low-energy expansion requires a loop expansion beyond lowest order [35]. But loop amplitudes have a tendency to be divergent. For a bona fide QFT we therefore need both regularization and renormalization. As strange as it may sound, also nonrenormalizable theories can and in fact must be renormalized to qualify as respectable QFTs.

A nonrenormalizable QFT like CHPT has many common features with the more standard renormalizable theories.

- ☛ Divergences are absorbed by the coupling constants in the higher-order Lagrangians  $\mathcal{L}_4, \mathcal{L}_6, \dots$ . Unlike in renormalizable theories, new LECs occur at every order of the chiral expansion.



- ✦ The renormalized LECs are scale dependent just like the strong coupling constant  $g_s(\mu)$ . They can be interpreted as describing the effect of all heavy hadronic states that are not represented by explicit fields in the Lagrangian.
- ✦ Renormalization ensures that there is no dependence on some artificial cutoff.

For phenomenological applications, we have to know the values of the various LECs. In principle, QCD fixes those constants but a matching between QCD and CHPT is not possible in perturbation theory. This was already discussed in Sec. 3.1 for general EFTs with SSB but it is also easy to understand in the present case: CHPT can only be applied for energies  $E \ll M_\rho$  whereas perturbative QCD only makes sense for  $E \gtrsim 1.5$  GeV. The most successful approaches bridging this gap to get information on the LECs are resonance saturation (based on the properties of QCD for large  $N_c$ , i.e. for a fictitious world with many colours) and lattice QCD.

The chiral expansion is an expansion in  $p^2/(4\pi F)^2$  where  $p$  is a characteristic momentum for the process in question. Therefore, the chiral expansion should and does work better for  $SU(2)$  than for  $SU(3)$ :

$$n_F = 2 : \frac{p^2}{(4\pi F)^2} = 0.014 \frac{p^2}{M_\pi^2} , \quad n_F = 3 : \frac{p^2}{(4\pi F)^2} = 0.18 \frac{p^2}{M_K^2} . \quad (151)$$

Most amplitudes and form factors for realistic processes have been calculated at least to next-to-leading order. There is an easy-to-use Mathematica program to generate both strong and nonleptonic weak transitions up to  $O(p^4)$  that is described in Ref. [36] and is available for general use. The state of the art is next-to-next-to-leading order or  $O(p^6)$ . A short introduction can be found in Ref. [33].

### 3.6 Light quark masses

In CHPT, the light quark masses always appear in the combination  $B m_q \sim m_q \langle 0 | \bar{u} u | 0 \rangle$ . Since there are no quarks or gluons in CHPT, only QCD scale invariant quantities can appear. As we discussed in Sec. 3.2, quark masses are scale dependent whereas the product  $m_q \langle 0 | \bar{u} u | 0 \rangle$  is not. The consequence is that CHPT can only provide methods for extracting the ratios of quark masses.

The lowest-order expressions for the meson masses in terms of quark masses can be read off directly from the Lagrangian (148):

$$\begin{aligned} M_{\pi^+}^2 &= 2\hat{m}B , & M_{\pi^0}^2 &= 2\hat{m}B + O[(m_u - m_d)^2/(m_s - \hat{m})] \\ M_{K^+}^2 &= (m_u + m_s)B , & M_{\eta_8}^2 &= \frac{2}{3}(\hat{m} + 2m_s)B + O[(m_u - m_d)^2/(m_s - \hat{m})] \\ M_{K^0}^2 &= (m_d + m_s)B , & \hat{m} &:= \frac{1}{2}(m_u + m_d) . \end{aligned} \quad (152)$$

Several well-known relations follow from these expressions:

$$\begin{aligned} \text{Gell-Mann-Oakes-Renner} & & F_\pi^2 M_\pi^2 &= -2\hat{m} \langle 0 | \bar{u} u | 0 \rangle \\ \text{GMOR, Weinberg} & & B &= \frac{M_\pi^2}{2\hat{m}} = \frac{M_{K^+}^2}{m_s + m_u} = \frac{M_{K^0}^2}{m_s + m_d} \\ \text{Gell-Mann-Okubo} & & 3M_{\eta_8}^2 &= 4M_K^2 - M_\pi^2 \quad (\text{isospin limit}) \end{aligned}$$

The relations (152) are also the basis for the so-called current algebra mass ratios

$$\frac{m_u}{m_d} = 0.55 , \quad \frac{m_s}{m_d} = 20.1 , \quad \frac{m_s}{\hat{m}} = 25.9 . \quad (153)$$

These ratios are subject to higher-order corrections, most importantly of  $O(p^4) = O(m_q^2)$  and  $O(e^2 m_s)$ . Because of an accidental symmetry at  $O(p^4)$ , the ratios  $m_s/m_d$ ,  $m_u/m_d$  cannot be extracted separately from S-matrix elements but only in the combination known as Leutwyler's ellipse [37] shown in Fig. 24.

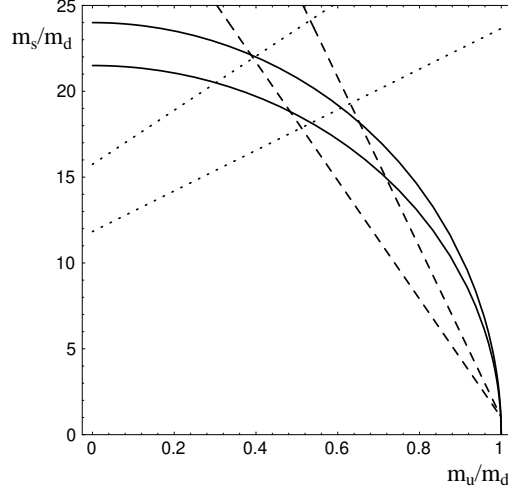


**Fig. 24:** Constraints on light quark mass ratios [37].

In addition to the full boundaries following directly from CHPT (the difference is due to uncertainties in the electromagnetic corrections), information is also available from  $\eta - \eta'$  mixing (dotted lines), baryon mass splittings and  $\rho - \omega$  mixing (dashed lines). The overall conclusion is that the corrections of  $O(p^4)$  are small for the ratios. The next-to-next-to-leading corrections of  $O(p^6)$  are also known [38] but there are at the moment too many unknown LECs for quantitative conclusions.

	$m_u/m_d$	$m_s/m_d$	$m_s/\hat{m}$
$O(p^2)$	0.55	20.1	25.9
$O(p^4)$	$0.55 \pm 0.04$	$18.9 \pm 0.8$	$24.4 \pm 1.5$

**Table 1:** Quark mass ratios to  $O(p^4)$  [37].

Absolute values of the quark masses are less well known than the ratios. The main methods are QCD sum rules and lattice simulations, most recently with full (unquenched) QCD. From the Review of Particle Properties [14], the combined result of lattice determinations of the strange quark mass is  $m_s(2 \text{ GeV}) = (100 \pm 25) \text{ MeV}$ . More results are reproduced in Fig. 18.

### 3.7 Pion pion scattering

Pion pion scattering has a privileged status in CHPT. It is **the** fundamental scattering process of CHPT and it involves only pions. The low-energy expansion can therefore be set up in the framework of chiral  $SU(2)$  and it can be expected to converge well. The scattering amplitude is very sensitive to the mechanism of spontaneous chiral symmetry breaking giving access to the quark condensate in particular.

The following review of recent developments will be restricted to the isospin limit ( $m_u = m_d$ ) in the absence of electromagnetic corrections. In this case, the information for all possible scattering channels is contained in a single amplitude  $A(s, t, u)$  (with  $s + t + u = 4M_\pi^2$ ).

The lowest-order amplitude of  $O(p^2)$  was already shown in Eq. (150):

$$A_2(s, t, u) = \frac{s - M_\pi^2}{F_\pi^2}.$$

At the same order, the quark mass ratio  $r = \frac{m_s}{\hat{m}} = \frac{2M_K^2}{M_\pi^2} - 1 \simeq 26$ , as also shown in Table 1. As the mass ratio  $r$ , also the S-waves are very sensitive to the quark condensate. In a modified version of CHPT

(Generalized CHPT [39]), one can tune the quark condensate. As an example, I show the leading-order results for the  $I = 0$  S-wave scattering length  $a_0^0$  and for the quark mass ratio  $r$  for both the standard and for a very small value of the quark condensate:

$a_0^0$	$r$	$B(\nu = 1 \text{ GeV})$
0.16	26	1.4 GeV (standard value)
0.26	10	$F_\pi$

At next-to-leading order, the scattering amplitude was calculated in 1983 [40]. It turns out that especially the S-wave scattering lengths are quite sensitive to chiral corrections (chiral logs). For instance,  $a_0^0$  increases from 0.16 at  $O(p^2)$  to 0.20 at  $O(p^4)$ , an increase of 25 % and thus quite a bit larger than the natural estimate in Eq. (151). Since the favoured experimental value of  $a_0^0$  at that time was 0.26 (with a 25 % error), it seemed mandatory to perform one more step in the chiral expansion. From the amplitude to  $O(p^6)$  [41] it was clear that a value  $a_0^0 = 0.26$  was not compatible with QCD. To narrow down the uncertainties related to the LECs appearing in the  $\pi\pi$  amplitude, the chiral amplitude was finally combined with dispersion theory (Roy equations) [42].

CHPT together with dispersion theory predicts not only the S-wave scattering lengths with amazing precision [42],

$$a_0^0 = 0.220 \pm 0.005, \quad a_0^2 = -0.0444 \pm 0.0010, \quad (154)$$

but also the S- and P-wave phase shifts. As a by-product, the ponium lifetime is predicted to be  $\tau = (2.9 \pm 0.1) \cdot 10^{-15}$ . A short history of the S-wave scattering lengths is shown in Fig. 25.

There is a small caveat here. All the results have been derived in the standard framework of CHPT that assumes a large quark condensate. With recent experimental information on the pion-pion phase shift difference  $\delta_0^0 - \delta_1^1$  from  $K_{e4}$  decays, even this last loophole could be closed. Using the correlation between  $a_0^2$  and  $a_0^0$  implied by the Roy equations, the measured phase shift difference [43] can be used to determine  $a_0^0$  as shown in Fig. 26. The fitted value [44]  $a_0^0 = 0.221 \pm 0.026$  is in perfect agreement with the prediction (154) from the combined analysis of CHPT and Roy equations.

The precise determination of the  $\pi\pi$  scattering amplitude has several important implications. One application concerns the chiral expansion of the pion mass in terms of the light quark masses  $m_u, m_d$ :

$$\begin{aligned} M_\pi^2 &= M^2 - \frac{\bar{l}_3}{32\pi^2 F^2} M^4 + O(M^6) \\ M^2 &= (m_u + m_d) |\langle 0 | \bar{u}u | 0 \rangle| / F^2. \end{aligned} \quad (155)$$

A by-product of the analysis of  $\pi\pi$  scattering is a precise determination of LECs like  $\bar{l}_3$ , which implies in turn that more than 94 % of  $M_\pi$  are in fact due to the leading term (the Gell-Mann–Oakes–Renner term) confirming the standard mechanism of spontaneous chiral symmetry breaking [44]. In other words, the

quark condensate is indeed the dominant order parameter of chiral symmetry breaking.

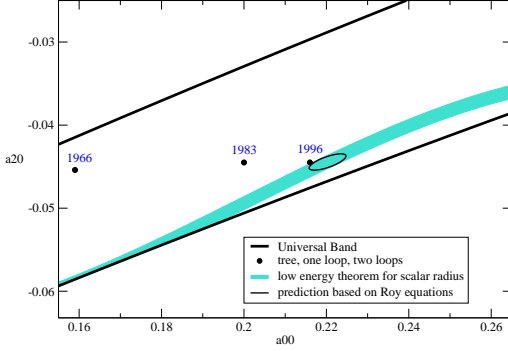


**Fig. 25:** Predictions for S-wave scattering lengths from current algebra till today, taken from Ref. [42].

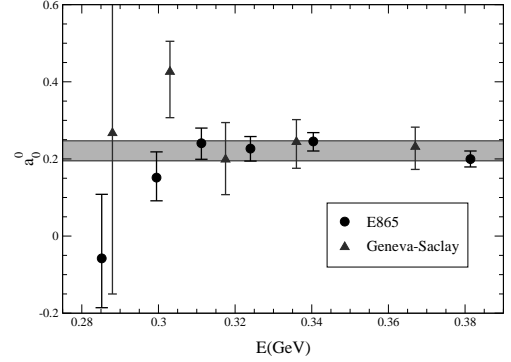


**Fig. 26:**  $K_{e4}$  data translated into a determination of the  $I = 0$  S-wave scattering length  $a_0^0$  [44].

The precise knowledge of the  $\pi\pi$  scattering amplitude from CHPT and dispersion theory has more recently (after the School) produced another important insight. The much discussed scalar isoscalar state now called  $f_0(600)$  by the Particle Data Group [14], but more commonly known as the  $\sigma$  meson, was analysed by Caprini, Colangelo and Leutwyler [45] by extending the Roy equations to complex values of the Mandelstam variable  $s$ . The result is an astonishingly precise determination of mass and width of the lightest hadronic resonance:

$$M_\sigma = 441_{-8}^{+16} \text{ MeV} , \quad \Gamma_\sigma = 544_{-18}^{+25} \text{ MeV} . \quad (156)$$

The  $\sigma$  resonance has the quantum numbers of the vacuum and it corresponds to an unambiguous pole on the second sheet of the scalar isoscalar partial wave. Its real part is close to threshold but the pole is quite far from the real axis. Although not as straightforward as its position in the complex energy plane, the most appealing interpretation of the  $\sigma$  is a quasi-bound state of two pions, quite different from a member of a standard  $\bar{q}q$  meson nonet [42, 45].

### 3.8 $K_{l3}$ decays and $V_{us}$

The Cabibbo–Kobayashi–Maskawa (CKM) matrix  $V_{ij}$  determines the structure of the hadronic charged weak current. The matrix elements are fundamental parameters of the Standard Model. Together with the quark and lepton masses, the CKM matrix and the corresponding lepton mixing matrix contain information about the mechanism of mass generation. Anticipating forthcoming LHC data to unveil the secrets of mass generation (Higgs sector), both masses and mixing angles should be measured as precisely as possible.

With three generations of quarks, the CKM matrix must be a unitary matrix. For some time, a possible problem with CKM unitarity has been discussed. With the PDG values of 2004 [14],

$$|V_{ud}| = 0.9738(5) , \quad |V_{us}| = 0.2200(26) , \quad (157)$$

unitarity appeared to be violated at the  $2.2 \sigma$  level by the elements of the first row  $V_{uj}$  ( $j = d, s, b$ ):

$$\sum_{j=d,s,b} |V_{uj}|^2 - 1 = -0.0033(15) . \quad (158)$$

At this level of accuracy, the element  $V_{ub}$  is still negligible. On the other hand, the required precision for  $V_{ud}$  and  $V_{us}$  calls for reliable isospin violating and electromagnetic corrections.

The most accurate determination of  $V_{us}$ , both experimentally and theoretically, comes from  $K_{l3}$  decays that can be treated in the framework of CHPT. The decay amplitude is governed by two form factors  $f_+(t)$  and  $f_-(t)$  with  $t = (p_K - p_\pi)^2$ :

$$\langle \pi^-(p_\pi) | \bar{s} \gamma_\mu u | K^0(p_K) \rangle = f_+^{K^0 \pi^-}(t) (p_K + p_\pi)_\mu + f_-^{K^0 \pi^-}(t) (p_K - p_\pi)_\mu . \quad (159)$$

Both form factors are known to next-to-next-to-leading order in CHPT. For the extraction of  $V_{us}$ , the crucial quantity is  $f_+(0)$ . The chiral expansion is of the form

$$f_+^{K^0 \pi^-}(0) = 1 + f_{p^4} + f_{e^2 p^2} + f_{p^6} + O[(m_u - m_d)p^4, e^2 p^4] . \quad (160)$$

The status of the various contributions is as follows:

$f_{p^4}$	−0.0227 (no uncertainty)	Gasser, Leutwyler [46]
$f_{e^2 p^2}$	radiative corrections	Cirigliano, Neufeld, Pichl [47]
$f_{p^6}$	loop contributions	Bijnens, Talavera [48]; Post, Schilcher [49]
	tree contributions	LECs $L_5^2$ , $C_{12} + C_{34}$

As a first test, we look at the ratio

$$r_{+0} = \left( \frac{2 \Gamma(K_{e3}^+(\gamma)) M_{K^0}^5 I_{K^0}}{\Gamma(K_{e3}^0(\gamma)) M_{K^+}^5 I_{K^+}} \right)^{1/2} = \frac{|f_+^{K^+ \pi^0}(0)|}{|f_+^{K^0 \pi^-}(0)|} . \quad (161)$$

This ratio is independent of  $f_{p^6}$  in Eq. (160) and it can therefore be predicted quite accurately [47, 50]:

$$r_{+0}^{\text{th}} = 1.023 \pm 0.003 , \quad (162)$$

to be compared with the experimental value [51]:

$$r_{+0}^{\text{exp}} = 1.036 \pm 0.008 . \quad (163)$$

What could be the origin of a possible discrepancy that is also suggested by the compilation of recent data in Fig. 27?

- In the past, radiative corrections have not always been state of the art. Nowadays, also experimentalists should only use the modern CHPT treatment [47].
- Measurements of the  $K^+$  and  $K_L$  lifetimes should still be improved.
- On the theory side, an unlikely but in principle still possible explanation could be that the error due to effects of  $O[(m_u - m_d)p^4, e^2 p^4]$  is underestimated.

The contribution  $f_{p^6}$  is the sum of a loop and of a tree-level part:

$$f_{p^6}^{L=1,2}(M_\rho) = 0.0093 \pm 0.0005 \quad \text{Bijnens, Talavera [46]} \quad (164)$$

$$\begin{aligned} f_{p^6}^{\text{tree}}(M_\rho) &= 8 \frac{(M_K^2 - M_\pi^2)^2}{F_\pi^2} \left[ \frac{(L_5^r(M_\rho))^2}{F_\pi^2} - C_{12}^r(M_\rho) - C_{34}^r(M_\rho) \right] \\ &= -\frac{(M_K^2 - M_\pi^2)^2}{2 M_S^4} \left( 1 - \frac{M_S^2}{M_P^2} \right)^2 . \end{aligned} \quad \begin{array}{l} \text{large-}N_c \text{ matching} \\ \text{Cirigliano et al. [52]} \end{array} \quad (165)$$

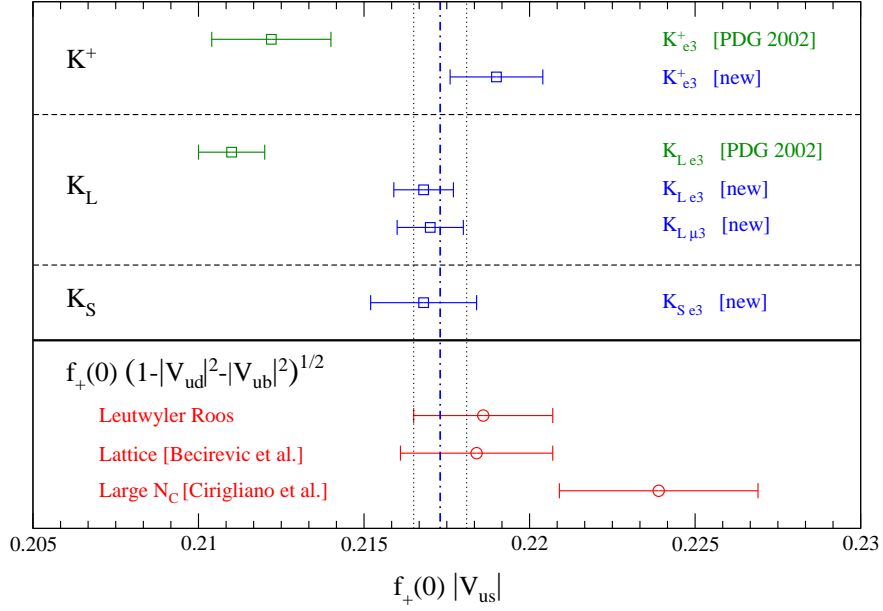


**Fig. 27:** Present experimental and theoretical status of  $f_+(0) |V_{us}|$  taken from Ref. [53].

The last equation is based on a large- $N_c$  estimate of Ref. [52]. As can be seen in Fig. 28, two terms interfere destructively weakening the overall dependence on the scalar resonance mass  $M_S$ . The same interference leads to a rather modest scale dependence of the result for  $M_\eta \leq \mu \leq 1$  GeV.

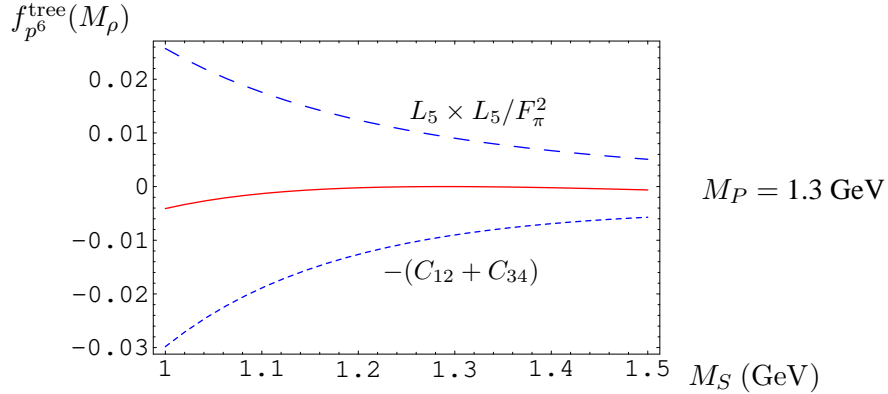


**Fig. 28:** Tree-level contribution of  $O(p^6)$  to  $f_+^{K^0\pi^-}(0)$  and its two components [52].

The final result, including the uncertainty due to a possible second pseudoscalar multiplet  $P'$ , is [52]

$$\begin{aligned}
 f_{p^6}^{\text{tree}}(M_\rho) &= -0.002 \pm 0.008_{1/N_c} \pm 0.002_{M_S} {}^{+0.000}_{-0.002} P' \\
 f_{p^6} &= 0.007 \pm 0.012 \\
 f_+^{K^0\pi^-}(0) &= 0.984 \pm 0.012.
 \end{aligned} \tag{166}$$

With our large- $N_c$  estimate of the tree-level contribution of  $O(p^6)$ ,  $f_{p^6}$  is dominated by the loop part (164). It exhibits less  $SU(3)$  breaking than the well-known result of Leutwyler and Roos [54] and a recent lattice estimate [55]. Taking the most recent value of  $V_{ud}$  and assuming unitarity of the CKM matrix, the predictions can be compared directly with the experimental results as shown in Fig. 27. A new result for the neutron lifetime [56] would imply a shift of all theoretical values in Fig. 27 to the left but

the corresponding accuracy of  $V_{ud}$  is not yet competitive with super-allowed nuclear Fermi transitions. Another way to read Fig. 27 is that the estimate of Ref. [52] leads to a value of  $V_{us}$ ,

$$|V_{us}| = 0.2208 \pm 0.0027_{f_+(0)} \pm 0.0008_{\text{exp}} , \quad (167)$$

that is a bit smaller than the unitarity prediction.

Finally, the slope of the scalar form factor that also depends on the LECs  $C_{12}, C_{34}$  can also be predicted [52] and it is in good agreement with the recent most precise experimental value [57]:

$$\begin{aligned} \lambda_0 &= (13 \pm 3) \cdot 10^{-3} && \text{Cirigliano et al. [52]} \\ \lambda_0 &= (13.72 \pm 1.31) \cdot 10^{-3} && \text{KTeV [57]} \end{aligned} \quad (168)$$

## 4 Summary and epilogue

There is an amazing richness contained in the simple Lagrangian that we “derived” from the existence of colour and from the gauge principle:

$$\mathcal{L}_{\text{QCD}} = -\frac{1}{2}\text{tr}(G_{\mu\nu}G^{\mu\nu}) + \sum_{f=1}^{N_F} \bar{q}_f (i\not{D} - m_f \mathbb{1}_c) q_f .$$

There is in fact no better summary for these lectures.

It may seem a long way from the naive quark model to QCD but it all happened in less than ten years. On the asymptotically free side, perturbative QCD is a complete success and it will be especially needed for understanding the background for new physics at the LHC and beyond.

There is much more left to be understood at the other end of the scale. If confinement is really forever, we would witness the first case in the history of physics when new constituents of matter have been identified beyond reasonable doubt and yet they can never be isolated. The question sounds preposterous but it is well supported: have we already arrived at the innermost structure of hadrons? Or put in a different way, is there no further structure to be expected before strings and quantum gravity eventually take over? In a short time, once the LHC will produce first results, we may learn how to rephrase the question.

## Acknowledgements

I want to thank both the organizers and the participants for creating such a lively and inspiring atmosphere during the School. Special thanks to Toni Pich for allowing me to use some of his figures in Ref. [58].

## References

- [1] D. J. Gross, Proc. Nat. Acad. Sci. **102** (2005) 9099;  
H. D. Politzer, Proc. Nat. Acad. Sci. **102** (2005) 7789;  
F. Wilczek, Proc. Nat. Acad. Sci. **102** (2005) 8403 [arXiv:hep-ph/0502113].
- [2] R.P. Feynman, in *The Quantum Theory of Fields - The 12th Solvay Conference* (Interscience, New York, 1961).
- [3] M. Gell-Mann, Phys. Lett. **8** (1964) 214;  
G. Zweig, CERN-TH.401.412 (1964) (unpublished).
- [4] M. Gell-Mann, Physics **1** (1964) 63.
- [5] A. Zee, Phys. Rev. D **7** (1973) 3630.
- [6] D. J. Gross and F. Wilczek, Phys. Rev. Lett. **30** (1973) 1343;  
H. D. Politzer, Phys. Rev. Lett. **30** (1973) 1346.

- [7] N. K. Nielsen, Am. J. Phys. **49** (1981) 1171.
- [8] H. Fritzsch and M. Gell-Mann, “Current algebra: quarks and what else?”, arXiv:hep-ph/0208010.
- [9] H. Fritzsch, M. Gell-Mann and P. Minkowski, Phys. Lett. B **59** (1975) 256.
- [10] S. Kluth, Nucl. Phys. Proc. Suppl. **133** (2004) 36 [arXiv:hep-ex/0309070].
- [11] V. V. Ezhela, S. B. Lugovsky and O. V. Zenin, “Hadronic part of the muon  $g-2$  estimated on the  $\sigma(\text{total})(2003)(e^+ e^- \rightarrow \text{hadrons})$  evaluated data compilation”, arXiv:hep-ph/0312114.
- [12] S. R. Coleman and D. J. Gross, Phys. Rev. Lett. **31** (1973) 851.
- [13] R.K. Ellis, W.J. Stirling and B.R. Webber, *QCD and Collider Physics* (Cambridge University Press, Cambridge, 2003).
- [14] S. Eidelman *et al.* [Particle Data Group], Phys. Lett. B **592** (2004) 1.
- [15] S. Bethke, Nucl. Phys. Proc. Suppl. **135** (2004) 345 [arXiv:hep-ex/0407021].
- [16] E. Braaten, S. Narison and A. Pich, Nucl. Phys. B **373** (1992) 581.
- [17] C. G. Callan and D. J. Gross, Phys. Rev. Lett. **22** (1969) 156.
- [18] A. Kappes [ZEUS Collaboration], “Structure function results from ZEUS”, arXiv:hep-ex/0210032.
- [19] V. N. Gribov and L. N. Lipatov, Sov. J. Nucl. Phys. **15** (1972) 438 [Yad. Fiz. **15** (1972) 781];  
L. N. Lipatov, Sov. J. Nucl. Phys. **20** (1975) 94 [Yad. Fiz. **20** (1974) 181];  
G. Altarelli and G. Parisi, Nucl. Phys. B **126** (1977) 298;  
Y. L. Dokshitzer, Sov. Phys. JETP **46** (1977) 641 [Zh. Eksp. Teor. Fiz. **73** (1977) 1216].
- [20] J. A. M. Vermaseren, A. Vogt and S. Moch, Nucl. Phys. B **724** (2005) 3 [arXiv:hep-ph/0504242].
- [21] J. Goldstone, Nuovo Cimento **19** (1961) 154.
- [22] A. V. Manohar and C. T. Sachrajda, “Quark masses”, in Ref. [14].
- [23] A. V. Manohar and M. B. Wise, *Heavy quark physics*, Camb. Monogr. Part. Phys. Nucl. Phys. Cosmol. **10** (2000) 1;  
T. Mannel, *Effective field theories in flavour physics*, Springer Tracts in Modern Physics **203** (Springer, Berlin 2004).
- [24] N. Brambilla *et al.*, “Heavy quarkonium physics”, arXiv:hep-ph/0412158.
- [25] M. Gourdin and E. de Rafael, Nucl. Phys. B **10** (1969) 667.
- [26] R. Alemany, M. Davier and A. Höcker, Eur. Phys. J. C **2** (1998) 123 [arXiv:hep-ph/9703220].
- [27] M. Davier, S. Eidelman, A. Höcker and Z. Zhang, Eur. Phys. J. C **31** (2003) 503 [arXiv:hep-ph/0308213].
- [28] V. Cirigliano, G. Ecker and H. Neufeld, Phys. Lett. B **513**, 361 (2001) [arXiv:hep-ph/0104267];  
JHEP **0208** (2002) 002 [arXiv:hep-ph/0207310].
- [29] A. Höcker, “The hadronic contribution to  $(g - 2)_\mu$ ”, arXiv:hep-ph/0410081.
- [30] K. Maltman, Phys. Lett. B **633** (2006) 512 [arXiv:hep-ph/0504201].
- [31] M. Davier and W. J. Marciano, Ann. Rev. Nucl. Part. Sci. **54** (2004) 115.
- [32] G. W. Bennett *et al.* [Muon  $g-2$  Collaboration], Phys. Rev. Lett. **92** (2004) 161802 [arXiv:hep-ex/0401008].
- [33] G. Ecker, Chiral perturbation theory, Lectures given at the Topical Seminar on Frontiers of Particle Physics: QCD and Light Hadrons, Beijing, China, Sept. 2004,  
<http://homepage.univie.ac.at/Gerhard.Ecker/beijingge.pdf>.
- [34] J. Gasser and H. Leutwyler, Ann. Phys. **158** (1984) 142; Nucl. Phys. B **250** (1985) 465.
- [35] S. Weinberg, Physica A **96** (1979) 327.
- [36] R. Unterdorfer and G. Ecker, JHEP **0510** (2005) 017 [arXiv:hep-ph/0507173].
- [37] H. Leutwyler, Phys. Lett. B **378** (1996) 313 [arXiv:hep-ph/9602366].



- [38] G. Amoros, J. Bijnens and P. Talavera, Nucl. Phys. B **602** (2001) 87 [arXiv:hep-ph/0101127].
- [39] J. Stern, “Light quark masses and condensates in QCD”, arXiv:hep-ph/9712438 and references therein.
- [40] J. Gasser and H. Leutwyler, Phys. Lett. B **125** (1983) 325.
- [41] J. Bijnens, G. Colangelo, G. Ecker, J. Gasser and M. E. Sainio, Phys. Lett. B **374** (1996) 210 [arXiv:hep-ph/9511397]; Nucl. Phys. B **508** (1997) 263 [Erratum-ibid. B **517** (1998) 639] [arXiv:hep-ph/9707291].
- [42] B. Ananthanarayan, G. Colangelo, J. Gasser and H. Leutwyler, Phys. Rept. **353** (2001) 207 [arXiv:hep-ph/0005297];  
G. Colangelo, J. Gasser and H. Leutwyler, Nucl. Phys. B **603** (2001) 125 [arXiv:hep-ph/0103088].
- [43] S. Pislak *et al.* [BNL-E865 Collaboration], Phys. Rev. Lett. **87** (2001) 221801 [arXiv:hep-ex/0106071]; Phys. Rev. D **67** (2003) 072004 [arXiv:hep-ex/0301040].
- [44] G. Colangelo, J. Gasser and H. Leutwyler, Phys. Rev. Lett. **86** (2001) 5008 [arXiv:hep-ph/0103063].
- [45] I. Caprini, G. Colangelo and H. Leutwyler, “Mass and width of the lowest resonance in QCD”, arXiv:hep-ph/0512364.
- [46] J. Gasser and H. Leutwyler, Nucl. Phys. B **250** (1985) 517.
- [47] V. Cirigliano, H. Neufeld and H. Pichl, Eur. Phys. J. C **35** (2004) 53 [arXiv:hep-ph/0401173].
- [48] J. Bijnens and P. Talavera, Nucl. Phys. B **669** (2003) 341 [arXiv:hep-ph/0303103].
- [49] P. Post and K. Schilcher, Eur. Phys. J. C **25** (2002) 427 [arXiv:hep-ph/0112352].
- [50] S. Descotes-Genon and B. Moussallam, Eur. Phys. J. C **42** (2005) 403 [arXiv:hep-ph/0505077].
- [51] H. Neufeld, private communication.
- [52] V. Cirigliano, G. Ecker, M. Eidemüller, R. Kaiser, A. Pich and J. Portolés, JHEP **0504** (2005) 006 [arXiv:hep-ph/0503108].
- [53] E. Blucher *et al.*, “Status of the Cabibbo angle (CKM2005 - WG 1)”, arXiv:hep-ph/0512039.
- [54] H. Leutwyler and M. Roos, Z. Phys. C **25** (1984) 91.
- [55] D. Becirevic *et al.*, Nucl. Phys. B **705** (2005) 339 [arXiv:hep-ph/0403217].
- [56] A. Serebrov *et al.*, Phys. Lett. B **605** (2005) 72 [arXiv:nucl-ex/0408009].
- [57] T. Alexopoulos *et al.* [KTeV Collaboration], Phys. Rev. D **70** (2004) 092007 [arXiv:hep-ex/0406003].
- [58] A. Pich, “Aspects of quantum chromodynamics”, arXiv:hep-ph/0001118.

## Bibliography

M.E. Peskin and D.V. Schroeder, *An Introduction to Quantum Field Theory* (Addison-Wesley, 1995).

J.F. Donoghue, E. Golowich and B.R. Holstein, *Dynamics of the Standard Model* (Cambridge University Press, Cambridge, 1994).

M.H. Seymour, *Quantum Chromodynamics*, Lectures given at the 2004 European School of High-Energy Physics, arXiv:hep-ph/0505192.

A. Khodjamirian, *QCD and Hadrons: an Elementary Introduction*, Lectures given at the 2003 European School of High-Energy Physics, arXiv:hep-ph/0403145.

Yu. L. Dokshitzer, *QCD Phenomenology*, Lectures given at the 2002 European School of High-Energy Physics, <http://doc.cern.ch/yellowrep/2004/2004-001/p1.pdf>.